JHEP

Published for SISSA by Springer

Received: May 2, 2017
Revised: August 11, 2017
Accepted: August 16, 2017
Published: September 4, 2017

Flavour anomalies after the R_{K^*} measurement

Guido D'Amico,[a] **Marco Nardecchia,**[a] **Paolo Panci,**[a] **Francesco Sannino,**[a,b] **Alessandro Strumia,**[a,c] **Riccardo Torre**[d,e] **and Alfredo Urbano**[a]

[a] *Theoretical Physics Department, CERN, CH-1211 Geneva, Switzerland*
[b] *CP^3-Origins and Danish IAS, University of Southern Denmark, Odense, Denmark*
[c] *Dipartimento di Fisica dell'Università di Pisa and INFN, Pisa, Italy*
[d] *Institut de Théorie des Phénomènes Physiques, EPFL, Route de la Sorge, CH-1015 Lausanne, Switzerland*
[e] *INFN, Sezione di Genova, Via Dodecaneso 33, I-16146 Genova, Italy*

E-mail: damico.guido@gmail.com, marco.nardecchia@cern.ch, paolo.panci@cern.ch, sannino@cp3.sdu.dk, astrumia@cern.ch, riccardo.torre@ge.infn.it, alfredo.leonardo.urbano@cern.ch

Abstract: The LHCb measurement of the μ/e ratio R_{K^*} indicates a deficit with respect to the Standard Model prediction, supporting earlier hints of lepton universality violation observed in the R_K ratio. We show that the R_K and R_{K^*} ratios alone constrain the chiralities of the states contributing to these anomalies, and we find deviations from the Standard Model at the 4σ level. This conclusion is further corroborated by hints from the theoretically challenging $b \to s\mu^+\mu^-$ distributions. Theoretical interpretations in terms of Z', lepto-quarks, loop mediators, and composite dynamics are discussed. We highlight their distinctive features in terms of the chirality and flavour structures relevant to the observed anomalies.

Keywords: Beyond Standard Model, Technicolor and Composite Models

ArXiv ePrint: 1704.05438

https://doi.org/10.1007/JHEP09(2017)010

JHEP09(2017)010

Contents

1 Introduction 1

2 Effective operators and observables 2
- 2.1 R_K revisited 3
- 2.2 Anatomy of R_{K^*} 4
- 2.3 $B_s \to \mu^+\mu^-$ 8

3 Fits 8
- 3.1 Fit to the 'clean' observables only 8
- 3.2 Fit to the 'hadronic sensitive' observables 11
- 3.3 Global fit 13

4 Theoretical interpretations 14
- 4.1 Models with an extra Z' 14
- 4.2 Models with lepto-quarks 16
- 4.3 Models with loop mediators 19
- 4.4 Fundamental composite Higgs 19

5 Conclusions 23

A List of observables used in the global fit 23

JHEP09(2017)010

1 Introduction

The LHCb [1] collaboration presented their results on the measurement of the ratio

$$R_{K^*} = \frac{\mathrm{BR}(B \to K^* \mu^+ \mu^-)}{\mathrm{BR}(B \to K^* e^+ e^-)} \,. \tag{1.1}$$

The aim of this measurement is to test the universality of the gauge interactions in the lepton sector. Taking the ratio of branching ratios strongly reduces the Standard Model (SM) theoretical uncertainties, as suggested for the first time in ref. [2].

The experimental result [1] is reported in two bins of di-lepton invariant mass

$$R_{K^*} = \begin{cases} 0.660^{+0.110}_{-0.070} \pm 0.024 & (2m_\mu)^2 < q^2 < 1.1\,\mathrm{GeV}^2 \\ 0.685^{+0.113}_{-0.069} \pm 0.047 & 1.1\,\mathrm{GeV}^2 < q^2 < 6\,\mathrm{GeV}^2 \,. \end{cases} \tag{1.2}$$

These values have to be compared with the SM predictions [3]

$$R^{SM}_{K^*} = \begin{cases} 0.906 \pm 0.028 & (2m_\mu)^2 < q^2 < 1.1\,\mathrm{GeV}^2 \\ 1.00 \pm 0.01 & 1.1\,\mathrm{GeV}^2 < q^2 < 6\,\mathrm{GeV}^2 \,. \end{cases} \tag{1.3}$$

At face value, a couple of observables featuring a $\sim 2.5\sigma$ deviation from the SM predictions can be attributed to a mere statistical fluctuation. The interest resides in the fact that such results might be part of a coherent picture involving New Physics (NP) in the $b \to s\mu^+\mu^-$ transitions. In fact, anomalous deviations were also observed in the following related measurements:

1. the R_K ratio [4]

$$R_K = \frac{\mathrm{BR}\left(B^+ \to K^+\mu^+\mu^-\right)}{\mathrm{BR}\left(B^+ \to K^+e^+e^-\right)} = 0.745 \pm 0.09_{\mathrm{stat}} \pm 0.036_{\mathrm{syst}}\,; \tag{1.4}$$

2. the branching ratios of the semi-leptonic decays $B \to K^{(*)}\mu^+\mu^-$ [5] and $B_s \to \phi\mu^+\mu^-$ [6];

3. the angular distributions of the decay rate of $B \to K^*\mu^+\mu^-$. In particular, the so-called P_5' observable (defined for the first time in [7]) shows the most significant discrepancy [5, 8, 9].

The coherence of this pattern of deviations has been pointed out already after the measurement of R_K with a subset of observables in [10, 11] and in a full global analysis in [12, 13].

For the observables in points 2 and 3 the main source of uncertainty is theoretical. It resides in the proper evaluation of the form factors and in the estimate of the non-factorizable hadronic corrections. Recently, great theoretical effort went into the understanding of these aspects, see refs. [7, 14–23] for an incomplete list of references.

Given their reduced sensitivity to theoretical uncertainties in the SM, the R_K and R_{K^*} observables offer a neat way to establish potential violation of lepton flavour universality. Future data will be able to further reduce the statistical uncertainty on these quantities. In addition, measurements of other ratios R_H analogous to R_K, with $H = X_s, \phi, K_0(1430), f_0$ will constitute relevant independent tests [2, 24].

The paper is structured as follows. In section 2 we discuss the relevant observables and how they are affected by additional effective operators. We perform a global fit in section 3. We show that, even restricting the analysis to the theoretically clean R_K, R_{K^*} ratios, the overall deviation from the SM starts to be significant, at the 4σ level, and to point towards some model building directions. Such results prompt us to investigate, in section 4, a few theoretical interpretations. We discuss models including Z', lepto-quark exchanges, new states affecting the observables via quantum corrections, and models of composite Higgs.

2 Effective operators and observables

Upon integrating out heavy degrees of freedom the relevant processes can be described, near the Fermi scale, in terms of the effective Lagrangian

$$\mathscr{L}_{\mathrm{eff}} = \sum_{\ell,X,Y} c_{b_X\ell_Y}\mathcal{O}_{b_X\ell_Y} \tag{2.1}$$

JHEP09(2017)010

where the sum runs over leptons $\ell = \{e, \mu, \tau\}$ and over their chiralities $X, Y = \{L, R\}$. New physics is more conveniently explored in the chiral basis

$$\mathcal{O}_{b_X \ell_Y} = (\bar{s}\gamma_\mu P_X b)(\bar{\ell}\gamma_\mu P_Y \ell). \tag{2.2}$$

These vector operators can be promoted to $\mathrm{SU}(2)_L$-invariant operators, unlike scalar or tensor operators [25]. In SM computations one uses the equivalent formulation

$$\mathscr{H}_{\rm eff} = -V_{tb}V_{ts}^* \frac{\alpha_{\rm em}}{4\pi v^2} \sum_{\ell,X,Y} C_{b_X \ell_Y} \mathcal{O}_{b_X \ell_Y} + \text{h.c.}\,, \tag{2.3}$$

defining dimensionless coefficients C_I as

$$c_I = V_{tb}V_{ts}^* \frac{\alpha_{\rm em}}{4\pi v^2} C_I = \frac{C_I}{(36\,\text{TeV})^2}\,, \tag{2.4}$$

where $V_{ts} = 0.040 \pm 0.001$ has a negligible imaginary part, $v = 174\,\text{GeV}$ is the Higgs vacuum expectation value, usually written as $1/v^2 = 4G_{\rm F}/\sqrt{2}$. The SM itself contributes as $C^{\rm SM}_{b_L\ell_L} = 8.64$ and $C^{\rm SM}_{b_L\ell_R} = -0.18$, accidentally implying $|C^{\rm SM}_{b_L\ell_R}| \ll |C^{\rm SM}_{b_L\ell_L}|$.

This observation suggests to use the chiral basis, related to the conventional one (see e.g. ref. [12]) by $C_9 = C_{b_L\mu_{L+R}}/2$, $C_{10} = -C_{b_L\mu_{L-R}}/2$, $C'_9 = C_{b_R\mu_{L+R}}/2$, $C'_{10} = -C_{b_R\mu_{L-R}}/2$, with the approximate relation $C_9^{\rm SM} \approx -C_{10}^{\rm SM}$ holding in the SM. To make the notation more compact, we define $C_{b_{L\pm R}\ell_Y} \equiv C_{b_L\ell_Y} \pm C_{b_R\ell_Y}$ and $C_{b_{L+R}\ell_{L\pm R}} \equiv C_{b_L\ell_L} + C_{b_R\ell_L} \pm C_{b_L\ell_R} \pm C_{b_R\ell_R}$, and $C_{b_X(\mu-e)_Y} \equiv C_{b_X\mu_Y} - C_{b_Xe_Y}$.

We now summarize the theoretically clean observables,[1] presenting both the full expressions and the ones in chiral-linear approximation. The latter is defined by neglecting $|C^{\rm SM}_{b_L\ell_R}| \ll |C^{\rm SM}_{b_L\ell_L}|$ and expanding each coefficient C_I at first order in the beyond-the-standard-model (BSM) contribution, $C_I = C_I^{\rm SM} + C_I^{\rm BSM}$.

2.1 R_K revisited

The experimental analysis is made by binning the observable in the squared invariant mass of the lepton system $q^2 \equiv (P_{\ell^-} + P_{\ell^+})^2$. Writing the explicit q^2-dependence, we have

$$R_K[q^2_{\rm min}, q^2_{\rm max}] \equiv \frac{\int_{q^2_{\rm min}}^{q^2_{\rm max}} dq^2 d\Gamma(B^+ \to K^+\mu^+\mu^-)/dq^2}{\int_{q^2_{\rm min}}^{q^2_{\rm max}} dq^2 d\Gamma(B^+ \to K^+e^+e^-)/dq^2}\,. \tag{2.5}$$

The experimental value cited in eq. (1.4) refers to $R_K \equiv R_K[1\ \text{GeV}^2, 6\ \text{GeV}^2]$. To simplify the notation, however, in the following we will omit the units in brackets. Neglecting SM contributions from the electromagnetic dipole operator, justified by the cut $q^2_{\rm min} = 1\,\text{GeV}^2$, and non-factorizable contributions from the weak effective Hamiltonian,[2] the theoretical prediction for R_K is

$$R_K = \frac{|C_{b_{L+R}\mu_{L-R}}|^2 + |C_{b_{L+R}\mu_{L+R}}|^2}{|C_{b_{L+R}e_{L-R}}|^2 + |C_{b_{L+R}e_{L+R}}|^2}\,. \tag{2.9}$$

[1] By theoretically clean observables we mean those ones predicted in the SM with an error up to few percent.

[2] In the limit of vanishing lepton masses the decay rate in eq. (2.5) takes the form [12]

$$\frac{d\Gamma(B^+ \to K^+\mu^+\mu^-)}{dq^2} = \frac{G_{\rm F}^2\alpha_{\rm em}^2|V_{tb}V_{ts}^*|^2}{2^{10}\pi^5 M_B^3}\lambda^{3/2}(M_B^2, M_K^2, q^2)\left(|F_V|^2 + |F_A|^2\right)\,, \tag{2.6}$$

JHEP09(2017)010

This is a clean observable, meaning that it is not affected by large theoretical uncertainties, and its SM prediction is $R_K = 1$. QED corrections give a small departure from unity which, however, does not exceed few percents [3]. However, it has to be noted that new physics which affects differently μ and e can induce theoretical errors, bringing back the issue of hadronic uncertainties.

In the chiral-linear approximation, R_K becomes

$$R_K \simeq 1 + 2\frac{\mathrm{Re}\, C^{\mathrm{BSM}}_{b_{L+R}(\mu-e)_L}}{C^{\mathrm{SM}}_{b_L\mu_L}}\,, \tag{2.10}$$

indicating that the dominant effect stems from couplings to left-handed leptons. Any chirality of quarks works, as long as it is not orthogonal to $L+R$, namely unless quarks are axial.

It is important to notice that the approximation in eq. (2.10), although capturing the relevant physics, is not adequate for a careful phenomenological analysis. The same remark remains valid for the simplified expression proposed in ref. [24], expanded up to quadratic terms in new physics coefficients. The reason is that the expansion is controlled by the parameter $C^{\mathrm{BSM}}_{b_X l_Y}/C^{\mathrm{SM}}_{b_X l_Y}$, a number that is not always smaller than 1. This is particularly true in the presence of new physics in the electron sector in which — as we shall discuss in detail — large values of the Wilson coefficients are needed to explain the observed anomalies. For this reason, all the results presented in this paper make use of the full expressions for both R_K [12] and, as we shall discuss next, R_{K^*}.

2.2 Anatomy of R_{K^*}

Given that the K^* has spin 1 and mass $M_{K^*} = 892\,\mathrm{MeV}$, the theoretical prediction for the R_{K^*} ratio given in eq. (1.1) is

$$R_{K^*} = \frac{(1-p)(|C_{b_{L+R}\mu_{L-R}}|^2 + |C_{b_{L+R}\mu_{L+R}}|^2) + p\left(|C_{b_{L-R}\mu_{L-R}}|^2 + |C_{b_{L-R}\mu_{L+R}}|^2\right)}{(1-p)(|C_{b_{L+R}e_{L-R}}|^2 + |C_{b_{L+R}e_{L+R}}|^2) + p\left(|C_{b_{L-R}e_{L-R}}|^2 + |C_{b_{L-R}e_{L+R}}|^2\right)} \tag{2.11}$$

where $p \approx 0.86$ is the "polarization fraction" [24, 27, 28], that is defined as

$$p = \frac{g_0 + g_\parallel}{g_0 + g_\parallel + g_\perp}\,. \tag{2.12}$$

The g_i are the contributions to the decay rate (integrated over the intermediate bin) of the different helicities of the K^*. The index i distinguishes the various helicities: longitudinal

where G_{F} is the Fermi constant, $\lambda(a,b,c) \equiv a^2+b^2+c^2-2(ab+bc+ac)$, $M_B \approx 5.279\,\mathrm{GeV}$, $M_K \approx 0.494\,\mathrm{GeV}$, $|V_{tb}V_{ts}^*| \approx 40.58 \times 10^{-3}$. Introducing the QCD form factors $f_{+,T}(q^2)$ we have

$$F_A(q^2) = \left(C_{10} + C'_{10}\right) f_+(q^2)\,, \tag{2.7}$$

$$F_V(q^2) = (C_9 + C'_9) f_+(q^2) + \underbrace{\frac{2m_b}{M_B + M_K}\left(C_7 + C'_7\right) f_T(q^2)}_{\text{SM electromagnetic dipole contribution}} + \underbrace{h_K(q^2)}_{\text{non-factorizable term}}\,. \tag{2.8}$$

Notice that for simplicity we wrote the Wilson coefficient C_9 omitting higher-order α_s-corrections [26]. Neglecting SM electromagnetic dipole contributions (encoded in the coefficients $C_7^{(\prime)}$), and non-factorizable corrections, eq. (2.9) follows from eqs. (2.5), (2.6) by rotating the coefficients $C_{9,10}^{(\prime)}$ on to the chiral basis.

JHEP09(2017)010

$(i = 0)$, parallel $(i = \|)$ and perpendicular $(i = \perp)$. In the chiral-linear limit the expression for R_{K^*} simplifies to

$$R_{K^*} \simeq R_K - 4p \frac{\mathrm{Re}\, C^{\mathrm{BSM}}_{b_R(\mu-e)_L}}{C^{\mathrm{SM}}_{b_L\mu_L}}\,, \tag{2.13}$$

where $4p/C^{\mathrm{SM}}_{b_L\mu_L} \approx 0.40$. The formula above clearly shows that, in this approximation, a deviation of R_{K^*} from R_K signals that b_R is involved at the effective operator level with the dominant effect still due to left-handed leptons. As already discussed before, eq. (2.13) is not suitable for a detailed phenomenological study, and we implement in our numerical code the full expression for R_{K^*} [29]. In the left panel of figure 1, we present the different predictions in the (R_K, R_{K^*}) plane due to turning on the various operators assumed to be generated via new physics in the muon sector. A reduction of the same order in both R_K and R_{K^*} is possible in the presence of the left-handed operator $C^{\mathrm{BSM}}_{b_L\mu_L}$ (red solid line). In order to illustrate the size of the required correction, the arrows correspond to $C^{\mathrm{BSM}}_{b_L\mu_L} = \pm 1$ (see caption for details). Conversely, as previously mentioned, a deviation of R_{K^*} from R_K signals the presence of $C^{\mathrm{BSM}}_{b_R\mu_L}$ (green dot-dashed line). Finally, notice that the reduced value of R_K measured in eq. (1.4) cannot be explained by $C^{\mathrm{BSM}}_{b_R\mu_R}$ and $C^{\mathrm{BSM}}_{b_L\mu_R}$. The information summarized in this plot is of particular significance since it shows at a glance, and before an actual fit to the data, the new physics patterns implied by the combined measurement of R_K and R_{K^*}.

Before proceeding, another important comment is in order. In the left panel of figure 1, we also show in magenta the direction described by non-zero values of the coefficient $C^{\mathrm{BSM}}_{9,\mu} = (C^{\mathrm{BSM}}_{b_L\mu_L} + C^{\mathrm{BSM}}_{b_L\mu_R})/2$. The latter refers to the effective operator $\mathcal{O}^\mu_9 = (\bar{s}\gamma_\mu P_L b)(\bar{\mu}\gamma^\mu\mu)$, and implies a vector coupling for the muon. The plot suggests that negative values $C^{\mathrm{BSM}}_{9,\mu} \approx -1$ may also provide a good fit of the observed data. However, it is also interesting to notice that in the non-clean observables, the hadronic effects might mimic a short distance BSM contribution in $C^{\mathrm{BSM}}_{9,\mu}$. From the plot in our figure 1, it is clear that with more data a combined analysis of R_K and R_{K^*} might start to discriminate between $C^{\mathrm{BSM}}_{9,\mu}$ and $C^{\mathrm{BSM}}_{b_L\mu_L}$ using *only* clean observables. However, with the present data, there is only a mild preference for $C^{\mathrm{BSM}}_{b_L\mu_L}$, according to the 1-parameter fits of section 3.1 using only clean observables.

It is also instructive to summarise in the right panel of figure 1 the case in which new physics directly affects the electron sector. The result is a mirror-like image of the muon case since the coefficients $C_{b_X e_Y}$ enter, both at the linear and quadratic level, with an opposite sign when compared to their analogue $C_{b_X\mu_Y}$. In the chiral-linear limit the only operator that can bring the values of R_K and R_{K^*} close to the experimental data is $C_{b_L e_L} > 0$. As before, a deviation from R_K in R_{K^*} can be produced by a non-zero value of $C^{\mathrm{BSM}}_{b_R e_L}$. Notice that, beyond the chiral-linear limit, also $C^{\mathrm{BSM}}_{b_{L,R} e_R}$ points towards the observed experimental data but they require larger numerical values.

A closer look to R_{K^*} reveals additional observable consequences related to the presence of BSM corrections. R_{K^*}, in a given range of q^2, is defined in analogy with eq. (2.5):

$$R_{K^*}[q^2_{\mathrm{min}}, q^2_{\mathrm{max}}] \equiv \frac{\int_{q^2_{\mathrm{min}}}^{q^2_{\mathrm{max}}} dq^2\, d\Gamma(B \to K^*\mu^+\mu^-)/dq^2}{\int_{q^2_{\mathrm{min}}}^{q^2_{\mathrm{max}}} dq^2\, d\Gamma(B \to K^*\mu^+\mu^-)/dq^2}\,, \tag{2.14}$$

JHEP09(2017)010

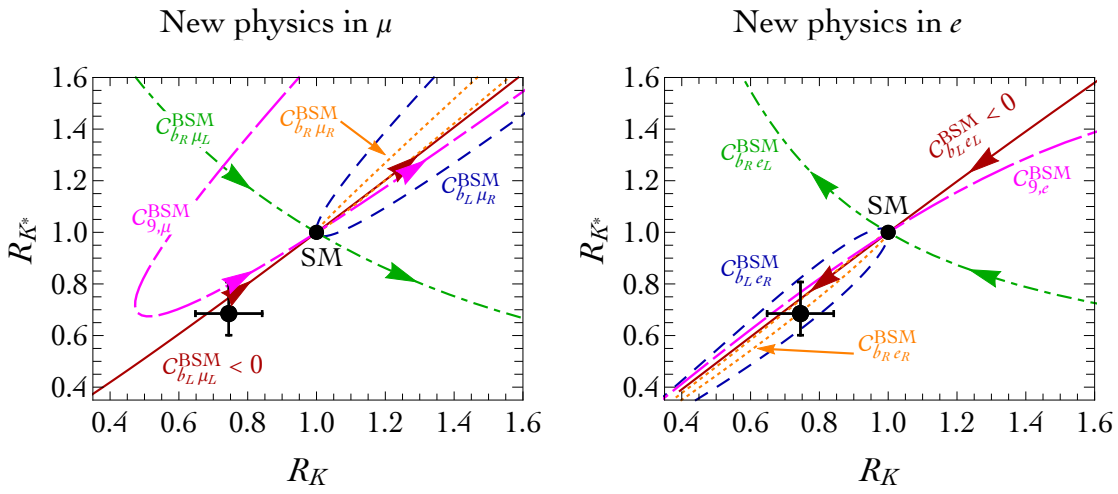

Figure 1. Deviations from the SM value $R_K = R_{K^*} = 1$ due to the various chiral operators possibly generated by new physics in the muon (left panel) and electron (right panel) sector. Both ratios refer to the $[1.1, 6]\,\text{GeV}^2$ q^2-bin. We assumed real coefficients, and the out-going (in-going) arrows show the effect of coefficients equal to $+1$ (-1). For the sake of clarity we only show the arrows for the coefficients involving left-handed muons and electrons (except for the two magenta arrows in the left-side plot, that refer to $C^{\rm BSM}_{9,\mu} = (C^{\rm BSM}_{b_L\mu_L} + C^{\rm BSM}_{b_L\mu_R})/2 = \pm 1$). The constraint from $B_s \to \mu\mu$ is not included in this plot.

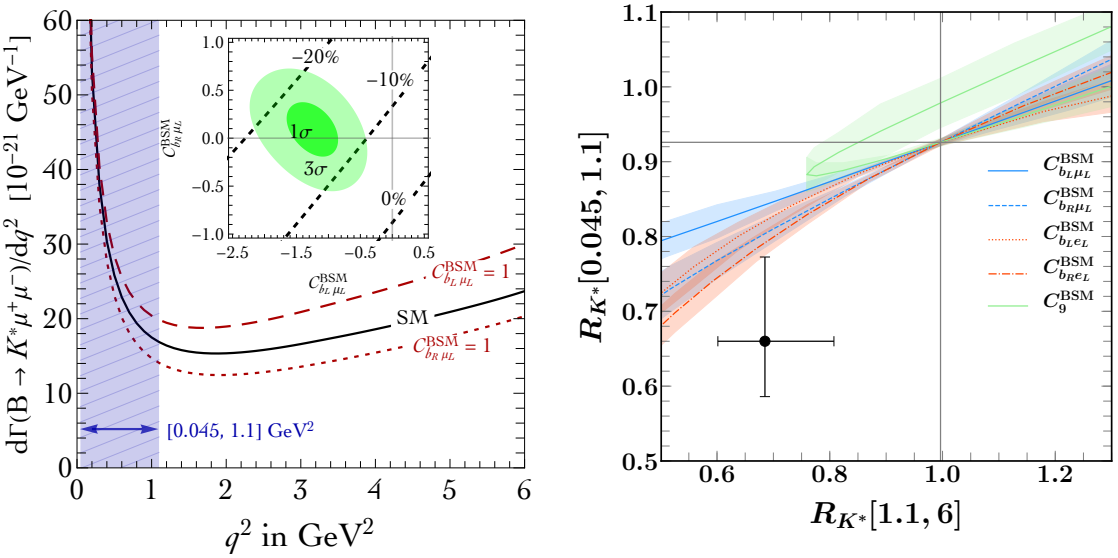

Figure 2. *Left:* R_{K^*} as function of q^2, the invariant mass of the $\ell^+\ell^-$ pair, for the SM and for two specific values of the new-physics coefficients. The inset shows iso-contours of deviation from $R^*_K = 1$ in the $[0.045, 1.1]\,\text{GeV}^2$ bin as a function of new-physics coefficients, compared to their experimentally favoured values. *Right:* correlation between R_{K^*} measured in the $[1.1, 6]\,\text{GeV}^2$ bin (horizontal axis) and $[0.045, 1.1]\,\text{GeV}^2$ bin (vertical axis) of q^2: a sizeable new physics effect can be present in the low-energy bin. The numerical values of q^2 are given in GeV^2.

JHEP09(2017)010

where the differential decay width $d\Gamma(B \to K^* \mu^+ \mu^-)/dq^2$ actually describes the four-body process $B \to K^*(\to K\pi)\mu^+\mu^-$, and takes the compact form

$$\frac{d\Gamma\left(B \to K^* \mu^+ \mu^-\right)}{dq^2} = \frac{3}{4}\left(2\mathcal{I}_1^s + \mathcal{I}_2^c\right) - \frac{1}{4}\left(2\mathcal{I}_2^s + \mathcal{I}_2^c\right) \ . \tag{2.15}$$

The angular coefficients $\mathcal{I}_{i=1,2}^{a=s,c}$ in eq. (2.15) can be written in terms of the so-called transversity amplitudes describing the decay $B \to K^* V^*$ with the B meson decaying to an on-shell K^* and a virtual photon or Z boson which later decays into a lepton-antilepton pair. We refer to ref. [29] for a comprehensive description of the computation. In the left panel of figure 2 we show the differential distribution $d\Gamma(B \to K^* \mu^+ \mu^-)/dq^2$ as a function of the dilepton invariant mass q^2. The solid black line represents the SM prediction, and we show in dashed (dotted) red the impact of BSM corrections due to the presence of non-zero $C_{b_L \mu_L}^{\rm BSM}$ ($C_{b_R \mu_L}^{\rm BSM}$) taken at the benchmark value of 1.

We now focus on the low invariant-mass range $q^2 = [0.045, 1.1]\,\text{GeV}^2$, shaded in blue with diagonal mesh in the left panel of fig 2. In this bin, the differential rate is dominated by the SM photon contribution. It is instructive to give more quantitative comments. In the inset plot in the left panel of fig 2, we show in the plane $(C_{b_L \mu_L}^{\rm BSM}, C_{b_R \mu_L}^{\rm BSM})$ the relative deviation in $R_{K^*}[0.045, 1.1]$ compared to its SM value $R_{K^*}^{\rm SM} \approx 0.9$, and we superimpose the 1- and 3-σ confidence contours allowed by the fit of experimental data (without including R_{K^*}). This comparison shows that a 10% reduction of R_{K^*} in the mass-invariant bin $q^2 = [0.045, 1.1]\,\text{GeV}^2$ is expected from the experimental data. The SM prediction, $R_{K^*}^{\rm SM}[0.045, 1.1] \approx 0.9$, departs from one because of QED effects which distinguish between m_μ and m_e. The observed central value $R_{K^*}^{\rm SM}[0.045, 1.1] = 0.66$ can be again explained with possible effects of new physics. The natural suspect is a new physics contribution to the dipole operator, but it can be shown that this cannot be very large because of bounds coming from the inclusive process $B \to X_s\gamma$, see for example ref. [30]. We can instead correlate the effect in $R_{K^*}^{\rm SM}[0.045, 1.1]$ with $R_{K^*}^{\rm SM}[1.1, 6]$. The results are shown in the right panel of figure 2. Here we learn that the new physics hypotheses predict values larger than the one observed in the data. However, since the experimental error is quite large, precise measurements are needed to settle this issue.

In conclusion, the picture emerging from a simple inspection of the relevant formulas for R_K and R_{K^*} is very neat, and can be summarized as follows:

- New physics in the muon sector can easily explain the observed deficits in R_K,R_{K^*}, and we expect a preference for negative values of the operator involving a left-handed current, $C_{b_L \mu_L}^{\rm BSM}$. Sizeable deviations of R_{K^*} from R_K signal non-zero values for $C_{b_R \mu_L}^{\rm BSM}$.

- New physics in the electron sector represents a valid alternative, and positive values of $C_{b_L e_L}^{\rm BSM}$ are favoured. Sizeable deviations of R_{K^*} from R_K signal non-zero values for $C_{b_R e_L}^{\rm BSM}$. However invoking NP only the electronic channels does not allow to explain other anomalies in the muon sector such as the angular observables.

- There exists an interesting correlation between R_{K^*} in the q^2-bin $[1.1, 6]\,\text{GeV}^2$ and $[0.045, 1.1]\,\text{GeV}^2$. At present, all the new physics hypothesis invoked tend to predicts larger value of R_{K*} in the low bin than the one preferred by the data.

In section 3 we shall corroborate this qualitative picture with quantitative fits.

JHEP09(2017)010

2.3 $B_s \to \mu^+\mu^-$

The rate is predicted as

$$\frac{\mathrm{BR}(B_s \to \mu^+\mu^-)}{\mathrm{BR}(B_s \to \mu^+\mu^-)_{\mathrm{SM}}} = \left| \frac{C_{b_{L-R}\mu_{L-R}}}{C^{\mathrm{SM}}_{b_{L-R}\mu_{L-R}}} \right|^2 , \tag{2.16}$$

where $\mathrm{BR}(B_s \to \mu^+\mu^-)_{\mathrm{SM}} = (3.65 \pm 0.23) \times 10^{-9}$ and $\mathrm{BR}(B_s \to \mu^+\mu^-)_{\mathrm{exp}} = (3.0 \pm 0.6) \times 10^{-9}$ [31]. This BR can also be affected by extra scalar operators $(\bar{b}P_X s)(\bar{\mu}P_Y \mu)$, so that it is sometimes omitted from global BSM fits.

3 Fits

We divide the experimental data in two sets: 'clean' and 'hadronic sensitive':

i) The 'clean' set includes the observables discussed in the previous section: R_K, R_{K^*}, to which one can add $\mathrm{BR}(B_s \to \mu^+\mu^-)$ given that it only provides constraints.[3] The 'cleanness' of these observables refers to the SM prediction, in the presence of New Physics larger theoretical uncertainties are expected. We didn't include the Q_4 and Q_5 observables measured recently by the Belle collaboration [33].

ii) The 'hadronic sensitive' set includes about 100 observables (summarized in the appendix A). This list includes the branching ratios of semi-leptonic B-meson decays as well as physical quantities extracted by the angular analysis of the decay products of the B-mesons. Concerning the hadronic sensitivity of the angular observables, the authors of [7] argue that the optimised variables P_i have reduced theoretical uncertainties.

The rationale is to first limit the analysis to the 'clean' set of observables. In this way one can draw solid conclusions without relying on large and partially uncontrolled effects. This approach is aligned with the spirit of this paper, and can be extremely powerful, as already shown in section 2.2. Furthermore, extracting from this reliable theoretical environment a BSM perspective could be of primary importance to set the stage for more complex analyses. In a second and third step we will estimate the effect of the 'hadronic sensitive' observables and combine all observables in a global fit.

3.1 Fit to the 'clean' observables only

The formulæ summarized in the previous section allow us to fit the clean observables. We wrote a dedicated Flavour Anomaly Rate Tool code (Fart). For simplicity, in our χ^2 fits we combine in quadrature the experimental errors on the two R_{K^*} bins, using the higher error band when they are asymmetric. We checked that our results do not change appreciably if a more precise treatment is used.

Let us start discussing the simplest case, in which we consider one-parameter fits to each NP operator in turn. Apart from its simplicity, this hypothesis is motivated from a

[3] When using the Flavio [32] code, for consistency we include the observable $\mathrm{BR}(B_0 \to \mu^+\mu^-)$, whose experimental error is correlated with the one on $\mathrm{BR}(B_s \to \mu^+\mu^-)$.

JHEP09(2017)010

theoretical viewpoint, as it captures most of the relevant features of concrete models, as we shall discuss in detail in section 4. We show the corresponding results — best-fit point, 1-σ error, and $\sqrt{\Delta\chi^2} \equiv \sqrt{\chi^2_{\rm SM} - \chi^2_{\rm best}}$ — in the 'clean' column in table 1. In the upper part of the table we show the cases in which we allow new physics in the muon sector. It is evident that the results of the fit match the discussion of section 2.2: the left-handed coefficient $C^{\rm BSM}_{b_L\mu_L}$ is favoured by the measured anomalies in R_K and R_{K^*}, with a significance of about 4σ. We can similarly discuss the hypothesis in which we allow for new physics in the electron sector, shown in the lower part of table 1. Three cases — $C^{\rm BSM}_{b_Le_L}$, $C^{\rm BSM}_{b_Le_R}$ and $C^{\rm BSM}_{b_Re_R}$ — are equally favoured by the fit. However, only the operator $\mathcal{O}_{b_Le_L}$ involving left-handed quarks and electrons can explain the observed anomalies with an order one Wilson coefficient since it dominates the new-physics corrections to both R_K and R_{K^*}, see eqs. (2.10), (2.13). As before, we find a statistical preference with respect to the SM case at the level of about 4-σ. To simplify the comparison with the existing literature, we show in table 2 the results of 1-parameter fits in the muon sector, this time in the vector-axial basis.

In conclusion, the piece of information that we learn from this simple fit is quite sharp: by restricting the analysis to the selected subset of 'clean' observables R_K, R_{K^*} and $\mathrm{BR}(B_s \to \mu^+\mu^-)$, not much affected by large theoretical uncertainties, we find a preference for the presence of new physics in the observed experimental anomalies in B decays. In particular, the analysis selects the existence of a new neutral current that couples left-handed b, s quarks and left-handed muons/electrons as the preferred option.

Effective four-fermions operators that couple left- or right-handed b, s with right-handed electrons are also equally preferred at this level of the analysis, but they require larger numerical values of their Wilson coefficients.

Needless to say, this conclusion, although already very significant, must be supported by the result of a more complete analysis that accounts for all the other observables related to B decays, and not included in the 'clean' set used in this section. We shall return to this point in section 3.2.

Before moving to the fit with the 'hadronic sensitive' observables, we perform several two-parameter fits using only 'clean' observables. We show our results in figure 3. Allowing for new physics in muons only, the combined best-fit regions are shown as yellow contours. Since there are few 'clean' observables, we turn on only two new-physics coefficients in each plot, as indicated on the axes. We also show, as rotated axes, the usual C_9 and C_{10} coefficients. We see that the key implications mentioned in section 2.2 are confirmed by this fit, although here wider regions in parameter space are allowed. In the upper plot of figure 3 we show the results for new physics in the operators involving left-handed muons, $C_{b_L\mu_L}$ and $C_{b_R\mu_R}$: both coefficients are fixed by the 'clean' data. Operators involving right-handed muons, on the other hand, do not lead to good fits. A good fit is obtained by turning on only $C_{b_L\mu_L}$, although uncertainties do not yet allow to draw sharp conclusions.

We conclude this section with a comment on the size of the theoretical uncertainties in the presence of New Physics. While there is a consensus on the small error of the Standard Model predictions, in the presence of New Physics the "clean" observables have a larger theoretical error, barring the special case where new physics violate flavour universality

JHEP09(2017)010

New physics in the muon sector									
Wilson	Best-fit			1-σ range			$\sqrt{\chi^2_{\rm SM} - \chi^2_{\rm best}}$		
coeff.	'clean'	'HS'	all	'clean'	'HS'	all	'clean'	'HS'	all
$C^{\rm BSM}_{b_L\mu_L}$	-1.27	-1.33	-1.30	-0.94 -1.62	-1.01 -1.68	-1.07 -1.55	4.1	4.6	6.2
$C^{\rm BSM}_{b_L\mu_R}$	0.64	-0.73	-0.30	1.17 0.11	-0.40 -1.03	0.02 -0.59	1.2	2.1	0.9
$C^{\rm BSM}_{b_R\mu_L}$	0.05	-0.20	-0.14	0.33 -0.23	-0.04 -0.29	0.00 -0.25	0.2	1.3	1.0
$C^{\rm BSM}_{b_R\mu_R}$	-0.44	0.41	0.27	0.08 -0.97	0.61 0.18	0.48 0.04	0.8	1.7	1.2
New physics in the electron sector									
Wilson	Best-fit			1-σ range			$\sqrt{\chi^2_{\rm SM} - \chi^2_{\rm best}}$		
coeff.	'clean'	'HS'	all	'clean'	'HS'	all	'clean'	'HS'	all
$C^{\rm BSM}_{b_Le_L}$	1.72	0.15	0.99	2.31 1.21	0.69 -0.39	1.30 0.70	4.1	0.3	3.5
$C^{\rm BSM}_{b_Le_R}$	-5.15	-1.70	-3.46	-4.23 -6.10	0.33 -2.83	-2.81 -4.05	4.3	0.9	3.6
$C^{\rm BSM}_{b_Re_L}$	0.085	-0.51	0.02	0.39 -0.21	0.29 -1.55	0.30 -0.25	0.3	0.7	0.1
$C^{\rm BSM}_{b_Re_R}$	-5.60	2.10	-3.63	-4.66 -6.56	3.52 -2.70	-2.65 -4.43	4.2	0.5	2.5

Table 1. Best fits assuming a single chiral operator at a time, and fitting only the 'clean' R_K, R_{K^*}, and BR($B_s \to \mu^+\mu^-$), or only the 'Hadronic Sensitive' observables (denoted by 'HS' in the table) as discussed in the text, or combining them in a global fit. The full list of observable can be find in appendix A.

while maintaining the same chiral structure of the SM (mostly LL at large enough q^2). As shown in figure 2, away from the Standard Model our errors are still of a few percent, in agreement with refs. [35, 36]. However, other groups [37] find a much larger theoretical error in the presence of New Physics, due to a more conservative treatment of the form factor uncertainties.[4] Therefore, we warn the reader that the statistical significance quoted in our fits may be smaller with a different treatment of the error.

We didn't take into account another important source of error: QED radiative corrections, calculated in ref. [3]. These are of the same order or larger than the hadronic uncertainties on R_K, R_{K*} in the Standard Model as predicted by FLAVIO. We did the

[4]We thank Joaquim Matias for enlightening discussions about this point.

JHEP09(2017)010

New physics in the muon sector (Vector Axial basis)									
Wilson	Best-fit			1-σ range			$\sqrt{\chi^2_{\rm SM} - \chi^2_{\rm best}}$		
coeff.	'clean'	'HS'	all	'clean'	'HS'	all	'clean'	'HS'	all
$C^{\rm BSM}_{9,\mu}$	-1.51	-1.15	-1.19	-1.05 -2.08	-0.98 -1.31	-1.04 -1.35	3.9	5.5	6.7
$C^{\rm BSM}_{10,\mu}$	0.97	0.48	0.66	1.28 0.69	0.69 0.28	0.83 0.50	3.8	2.4	4.3
$C'^{\rm BSM}_{9,\mu}$	-0.08	-0.24	-0.22	0.20 -0.37	0.44 -0.15	-0.14 -0.33	0.3	1.7	1.6
$C'^{\rm BSM}_{10,\mu}$	-0.11	0.10	0.07	0.11 -0.34	0.19 0.01	0.15 -0.01	0.5	1.2	0.9

Table 2. Same as table 1, but in the vector-axial basis.

exercise of inflating our hadronic error by a factor of 3, finding indeed a larger error away from the Standard Model, but still of the same order of the QED corrections.

3.2 Fit to the 'hadronic sensitive' observables

In order to perform a global fit using the 'hadronic sensitive' observables we use the public code Flavio [32].

Theoretical uncertainties are dominant, and it is difficult to quantify them. We first take theoretical uncertainties into account using the 'FastFit' method in the Flavio code with the addition of all the included nuisance parameters. With this choice, the SM is disfavoured at about 5σ level.

Given that most 'hadronic sensitive' observables involve muons (detailed measurements are much more difficult with electrons), we present a simple χ^2 of the 4 Wilson coefficients involving muons. This is a simple useful summary of the full analysis. In this approximation, the 'hadronic sensitive' observables determine the 4 muon Wilson coefficients as[5]

$$\begin{aligned} C^{\rm BSM}_{b_L\mu_L} &= -1.33 \pm 0.26 \\ C^{\rm BSM}_{b_R\mu_L} &= +0.29 \pm 0.31 \\ C^{\rm BSM}_{b_L\mu_R} &= -0.51 \pm 0.39 \\ C^{\rm BSM}_{b_R\mu_R} &= +0.45 \pm 0.93 \end{aligned} \qquad \text{with} \qquad \rho = \begin{pmatrix} 1 & -0.07 & 0.13 & 0.03 \\ -0.07 & 1 & 0.25 & 0.74 \\ 0.13 & 0.25 & 1 & 0.50 \\ 0.03 & 0.74 & 0.50 & 1 \end{pmatrix}. \tag{3.1}$$

The uncertainties can be rescaled by factors of $\mathcal{O}(1)$, if one believes that theoretical uncertainties should be larger or smaller than those adopted here.

The global fit of 'hadronic sensitive' observables to new physics in the 4 muon coefficients is also shown as red regions in figure 3. The important message is apparent both from

[5] In general, within the Gaussian approximation, the mean values μ_i, the errors σ_i and the correlation matrix ρ_{ij} determine the χ^2 as $\chi^2 = \sum_{i,j}(C_i - \mu_i)(\sigma^2)^{-1}_{ij}(C_j - \mu_j)$, where $(\sigma^2)_{ij} = \sigma_i \rho_{ij} \sigma_j$.

JHEP09(2017)010

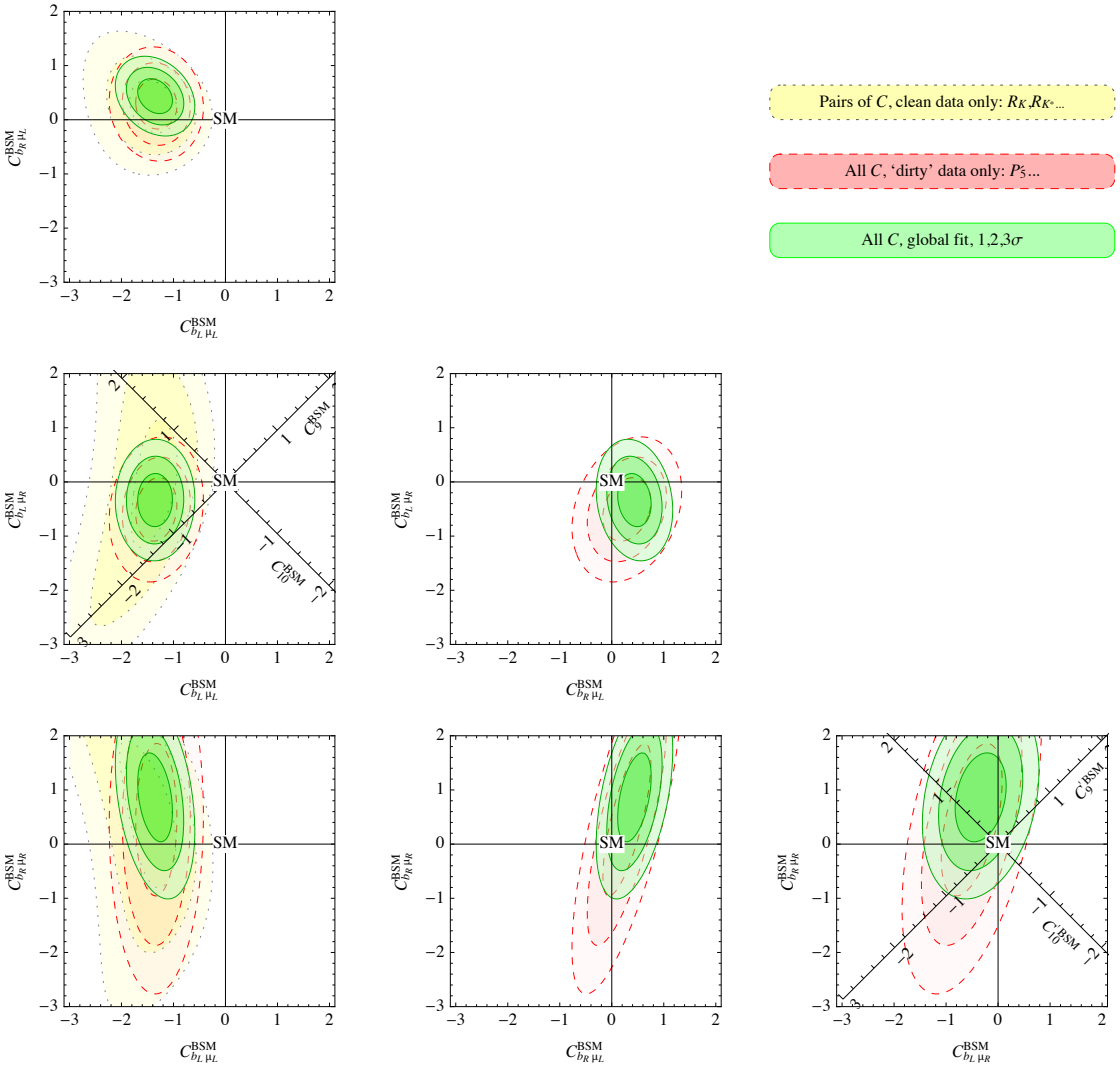

Figure 3. Fit to the new-physics contribution to the coefficients of the 4 muon operators $(\bar{b}\gamma_\mu P_X s)(\bar{\mu}\gamma_\mu P_Y \mu)$, showing the $1, 2, 3\sigma$ contours. The yellow regions with dotted contours show the best fit to the 'clean' observables only; due to the scarcity of data, in each plot we turn on only the two coefficients indicated on its axes. The red regions with dashed contours show the best global fit to the 'hadronic sensitive' observables only, according to one estimate of their theoretical uncertainties; in this fit, we turn on all 4 muon operators at the same time and, in each plot, we marginalise over the coefficients not shown in the plot. The green regions show the global fit, again turning on all 4 muon operators at the same time. In figure 5 we turn on the extra 4 electron operators too.

JHEP09(2017)010

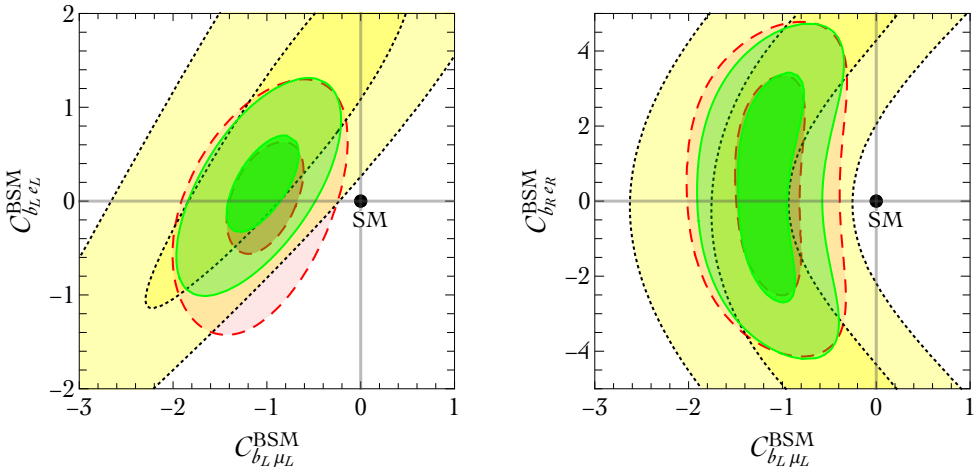

Figure 4. Fits allowing one operator involving muons (horizontal axis) and one involving electrons (vertical axis): left-handed in the left panel, and right-handed in the right panel. Regions and contours have the same meaning as in figure 3: 'clean' data can be fitted by an anomaly in muons or electrons; 'hadronic sensitive' data favour an anomaly in muons.

the figure and from eq. (3.1): *'hadronic sensitive' observables favour a deviation from the SM in the same direction as the 'clean' observables*, i.e. a negative contribution $C^{\rm BSM}_{b_L\mu_L} \sim -1$ to the Wilson coefficient involving left-handed quarks and muons. 'Clean' observables and 'hadronic sensitive' observables — whatever their uncertainty is — look consistent and favour independently the same pattern of deviations from the SM.

3.3 Global fit

We are now ready to combine 'clean' and 'hadronic sensitive' observables in a global fit, using both the FLAVIO and FART codes. The result is shown as green regions in figure 3, assuming that new physics affects muons only. The global fit favours a deviation in the SM in $C^{\rm BSM}_{b_L\mu_L}$, and provides bounds on the other new-physics coefficients. Using the Gaussian approximation for the likelihood of the muon coefficients, the global fit is summarized as

$$\begin{aligned} C^{\rm BSM}_{b_L\mu_L} &= -1.35 \pm 0.22 \\ C^{\rm BSM}_{b_R\mu_L} &= +0.44 \pm 0.21 \\ C^{\rm BSM}_{b_L\mu_R} &= -0.33 \pm 0.33 \\ C^{\rm BSM}_{b_R\mu_R} &= +0.86 \pm 0.54 \end{aligned} \qquad \text{with} \qquad \rho = \begin{pmatrix} 1 & -0.26 & 0.02 & -0.33 \\ -0.26 & 1 & -0.17 & 0.47 \\ 0.02 & -0.17 & 1 & 0.25 \\ -0.33 & 0.47 & 0.25 & 1 \end{pmatrix}. \tag{3.2}$$

An anomaly in muons is strongly preferred to an anomaly in electrons, if we adopt the default estimate of the theoretical uncertainties by FLAVIO. This is for example shown in figure 4, where we allow for a single operator involving muons and a single operator involving electrons.

In view of this preference, and given the scarcity of data in the electron sector, we avoid presenting a global fit of new physics in electrons only. We instead perform a global com-

JHEP09(2017)010

bined fit for the muon and electron coefficients (which should be interpreted with caution, given that 'hadronic sensitive' observables are dominated by theoretical uncertainties). We find the result shown in figure 5, which confirms that — while electrons can be affected by new physics — 'hadronic sensitive' data favour an anomaly in muons.

The latter result has been obtained by a global Bayesian fit to the observables listed in tables 6, 7 in addition to the clean observables. We used the FLAVIO code to calculate the likelihood, and we sampled the posterior using the EMCEE code [38], assuming for the 8 Wilson coefficients (at the scale 160 GeV) a flat prior between −10 and 10. In this global fit, we choose to marginalize over 25 nuisance parameters only, to keep computational times within reasonable limits. The nuisances (form factors related to B decays) are selected in the following way. For each observable, we define theoretical uncertainties due to changing each nuisance within its uncertainty, keeping the others fixed at their central values. Then, we choose to marginalize only over the parameters which give a theoretical uncertainty larger than the experimental error on the observable.

4 Theoretical interpretations

We now discuss different theoretical interpretations that can accommodate the flavour anomalies. We start with the observation that an effective $(\bar{s}\gamma_\mu P_X b)(\bar{\ell}\gamma_\mu P_Y \ell)$ interaction can be mediated at tree level by two kinds of particle: a Z' or a leptoquark. Higher-order induced mechanisms are also possible. These models tend to generate related operators

$$c_{b_L b_L}(\bar{s}\gamma_\mu P_L b)^2 + c_{\mu_L \nu_\mu}(\bar{\mu}\gamma^\mu P_L \mu)(\bar{\nu}_\mu \gamma_\mu P_L \nu_\mu)\,, \tag{4.1}$$

and therefore one needs to consider the associated experimental constraints. The first operator affects B_s mass mixing for which the relative measurements, together with CKM fits, imply $c^{\rm BSM}_{b_L b_L} = (-0.09 \pm 0.08)/(110\,{\rm TeV})^2$, i.e. the bound $|c^{\rm BSM}_{b_L b_L}| < 1/(210\,{\rm TeV})^2$ [11, 39]. The second operator is constrained by CCFR data on the neutrino trident cross section, yielding the weaker bound $|c^{\rm BSM}_{\mu_L \nu_\mu}| < 1/(490\,{\rm GeV})^2$ at 95% C.L. [40]. Furthermore, new physics that affects muons can contribute to the anomalous magnetic moment of the muon. Experiments found hints of a possible deviation from the Standard Model with $\Delta a_\mu = (24 \pm 9) \cdot 10^{-10}$ [41].

4.1 Models with an extra Z'

Models featuring extra Z' to explain the anomalies are very popular, see the partial list of references [42–61]. Typically these models contain a Z' with mass $M_{Z'}$ savagely coupled to

$$[g_{bs}(\bar{s}\gamma_\mu P_L b) + \text{h.c.}] + g_{\mu_L}(\bar{\mu}\gamma_\mu P_L \mu)\ . \tag{4.2}$$

The model can reproduce the flavour anomalies with $c_{b_L \mu_L} = -g_{bs} g_{\mu_L}/M^2_{Z'}$ as illustrated in figure 6a. At the same time the Z' contributes to the B_s mass mixing with $c_{b_L b_L} = -g^2_{bs}/2M^2_{Z'}$. The bound from ΔM_{B_s} can be satisfied by requiring a large enough g_{μ_L} in order to reproduce the $b \to s\ell^+\ell^-$ anomalies. Left-handed leptons are unified in a $\mathrm{SU}(2)_L$ doublet $L = (\nu_L, \ell_L)$, such that also the neutrino operator $c_{\mu_L \nu_\mu} = -g^2_{\mu_L}/M^2_{Z'}$ is generated. However the latter does not yield a strong constraint on g_{μ_L}.

JHEP09(2017)010

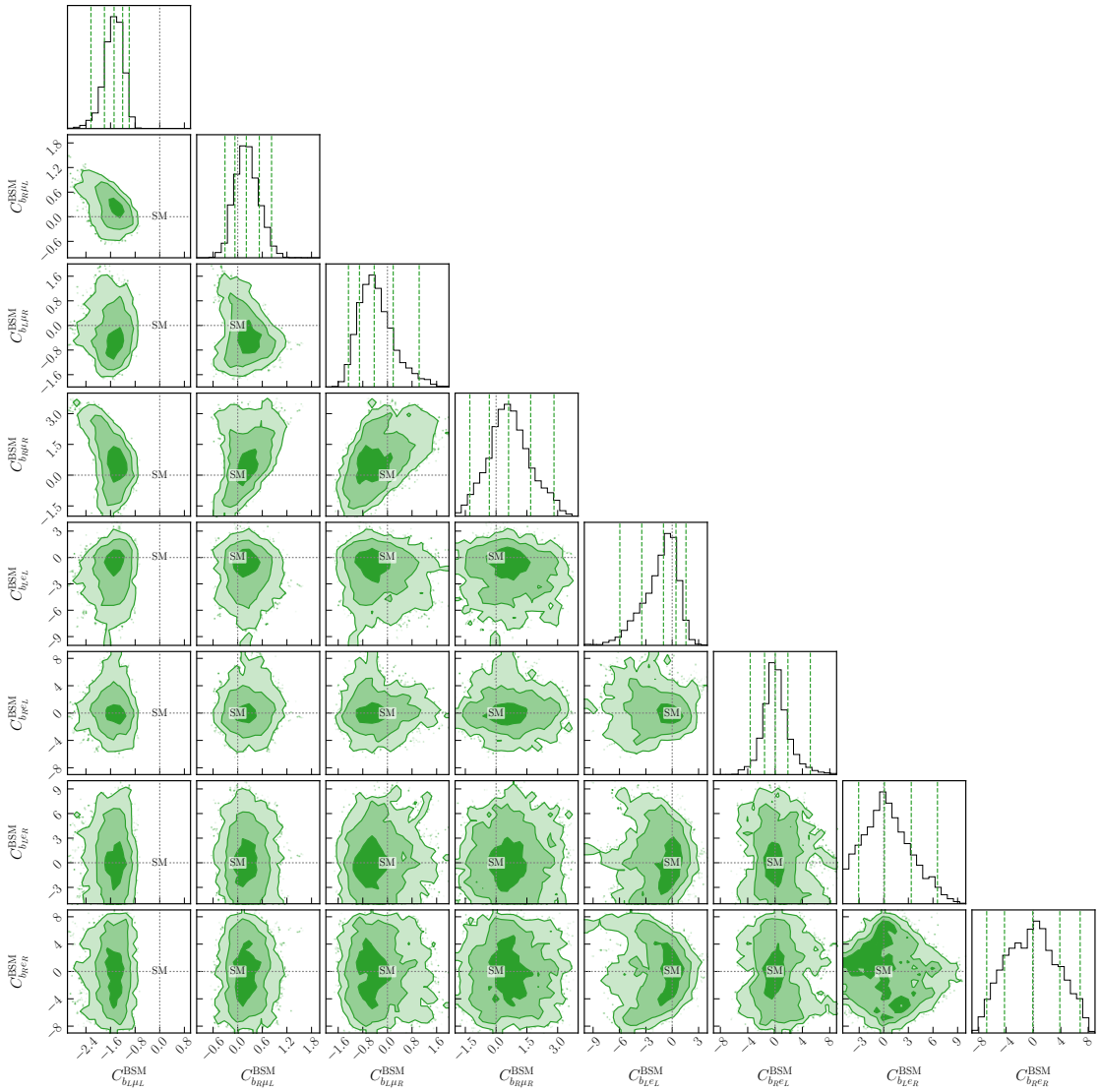

Figure 5. Global fit to the 8 Wilson coefficients in muons and electrons, combining 'clean' and 'hadronic sensitive' data.

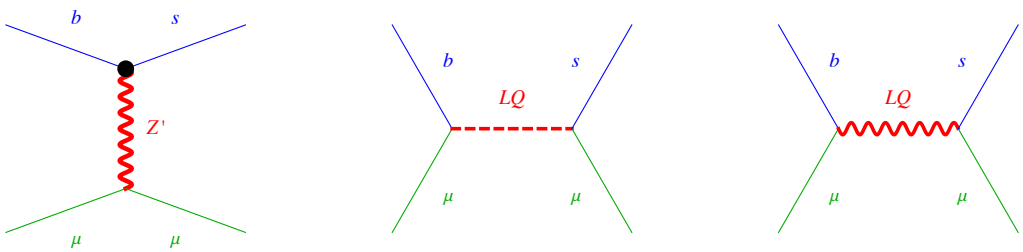

Figure 6. Particles that can mediate R_K at tree level: a Z' or a lepto-quark, scalar or vector.

JHEP09(2017)010

Another possibility is for the Z' to couple to the 3-rd generation left-handed quarks with coupling g_t and to lighter left-handed quarks with coupling g_q. The coupling g_{bs} arises as $g_{bs} = (g_t - g_q)(U_{Q_d})_{ts}$ after performing a flavour rotation U_{Q_d} among left-handed down quarks to their mass-eigenstate basis. The matrix element $(U_{Q_d})_{ts}$ is presumably not much larger than V_{ts} and possibly equal to it, if the CKM matrix $V = U_{Q_u} U_{Q_d}^\dagger$ is dominated by the rotation among left-handed down quarks, rather than by the rotation U_{Q_u} among left-handed up quarks.

Unless $g_q = 0$, the parameter space of the Z' model gets severely constrained by combining perturbative bounds on g_{μ_L}. In addition the LHC bounds on $pp \to Z' \to \mu\bar{\mu}$ can be relaxed by introducing extra features, such as a Z' branching ratio into invisible DM particles [62].

A characteristic feature of Z' models is that they can mediate effective operators involving different chiralities. In fact, gauge-anomaly cancellations also induce multiple chiralities: for example a Z' coupled to $L_\mu - L_\tau$ is anomaly free [44], where the L_e contribution is avoided because LEP put strong constraints on 4-electron operators. The chiralities involved in the $b \to s\ell^+\ell^-$ anomalies can be determined trough more precise measurements of 'clean' observables such as R_K and R_{K^*}.

4.2 Models with lepto-quarks

The anomalous effects in $b \to s\ell^+\ell^-$ transitions might be due to the exchange of a Lepto-Quark (LQ), namely a boson that couples to a lepton and a quark. Concerning lepton flavour, in general a LQ can couple to both muons and electrons. However, simultaneous sizeable couplings of a LQ to electrons and muons generates lepton flavour violation which is severely constrained by the time-honoured radiative decay $\mu \to e\gamma$. For this reason one typically assumes that LQs couple to either electrons or muons. (Here sizeable means an effect which has an impact on the anomalous observables). The coupling to muons allows to fit the anomalies in $b \to s\mu^+\mu^-$ distributions, as well as the R_K and R_{K^*} μ/e ratios.

The gauge quantum numbers of *scalar* LQs select a specific chirality of the SM fermions involved in the new Yukawa couplings, and thereby generate a unique characteristic operator in the effective Lagrangian in the chiral basis of eq. (2.1), as illustrated in figure 6b. The correspondence is given by

Coefficient	Lepto-Quark	Yukawa couplings
$C_{b_L\ell_L}$	$S_3 \sim (\bar{3}, 3, 1/3)$	$y\, QL\, S_3 + y'\, QQ\, S_3^\dagger + \text{h.c.}$
$C_{b_L\ell_R}$	$R_2 \sim (3, 2, 7/6)$	$y\, UL\, R_2 + y'\, QE\, R_2^\dagger + \text{h.c.}$
$C_{b_R\ell_L}$	$\tilde{R}_2 \sim (3, 2, 1/6)$	$y\, DL\, \tilde{R}_2 + \text{h.c.}$
$C_{b_R\ell_R}$	$\tilde{S}_1 \sim (\bar{3}, 1, 4/3)$	$y\, DE\, \tilde{S}_1 + y'\, UU\, \tilde{S}_1^\dagger + \text{h.c.}$

(4.3)

where ℓ can be either an electron or a muon. In parentheses we report the SU(3) $\times$ SU(2)$_L$ $\times$ U(1)$_Y$ gauge quantum numbers, and we follow the notations and conventions from ref. [63] for LQ names. Q, L (U, D, E) denote the left-handed (right-handed) SM quarks and leptons.

JHEP09(2017)010

Given that each LQ mediates effective operators with a given chirality, we can draw conclusions from our one parameter fits of the $b \to s\ell^+\ell^-$ anomalies of table 1. Assuming new physics in the muon sector, the measurement of R_{K^*} selects a unique scalar leptoquark: $S_3 \sim (\bar{3}, 3, 1/3)$, which is a triplet under $\mathrm{SU}(2)_L$. It is remarkable that this is obtained with just the information coming from 'clean' observables while the inclusion of the remaining observables (with our specified treatment of the errors) reinforces this hypothesis. The explanation of the anomalies in terms of S_3 has been firstly proposed after the measurement of R_K in ref. [10] switching on only those couplings needed to reproduce the effect. In ref. [64] the LQ has been identified as a pseudo-Goldstone boson associated to the breaking of a global symmetry of a new strongly coupled sector [65]. In refs. [64, 65] it has also been suggested that a rationale for the size of the various flavour couplings could be dictated by the mechanism of partial compositeness [66]. Another motivated pattern of couplings has been suggested in ref. [67] using flavour symmetry. Also ref. [68] makes use of S_3 as mediator of the $b \to s\mu^+\mu^-$ transition.

A potential issue with S_3 is the danger of extra renormalizable couplings with diquarks (denoted collectively by y' in the Lagrangians above) which may induce proton decay. Baryon number conservation has to be invoked to avoid this issue. Motivated by this, in refs. [69, 70], the LQ $\tilde{R}_2$ (which respects the global symmetry $\mathrm{U}(1)_B$ accidentally at the renormalizable level) has been considered leading to the prediction $R_{K^*} > 1$, which is now disfavoured by the LHCb data. The other two options $\tilde{S}_1$ and R_2 were already disfavoured after the measurement of R_K [10, 71].

The situation is different if LQs couple to electrons, rather than to muons, such that only the anomalies in the 'clean' observables can be reproduced. 'Clean' observables can be reproduced by all chiralities, with the only exclusion of $C_{b_R\ell_L}$, which is mediated by the $\tilde{R}_2$ LQ. From the fit, we notice that the $\tilde{S}_1$ and R_2 LQs can only fit the anomalies by giving a large contribution to the Wilson coefficients, comparable to the SM contributions: this happens because these LQs couple to right handed electrons, with little interference with the SM. One the other hand, S_3 couples to left-handed leptons, such that the sizeable interference with the SM allows to reproduce the observed anomalies with a smaller new physics component.

We briefly comment on the possible interpretation of a LQ as a supersymmetric particle in the MSSM. The only sparticle with the same gauge quantum numbers as a LQ is the left-handed squark $\tilde{Q} \sim \tilde{R}_2$. However, even if it has R-parity violating interactions, this LQ gives the wrong correlation between R_K and R_{K^*}, disfavouring the supersymmetric interpretation of the anomalies.

We move now to the discussion of the exchange of *vector* LQs at tree level, illustrated in figure 6c. There are 3 cases: $U_3 \sim (3, 3, 2/3)$, $V_2 \sim (\bar{3}, 2, 5/6)$ and $U_1 \sim (\bar{3}, 1, 2/3)$. Their relevant interactions are:

$$\mathscr{L}_{U_3} = y\, \bar{Q}\gamma_\mu L\, U_3^\mu + \text{h.c.} \tag{4.4a}$$

$$\mathscr{L}_{V_2} = y\, \bar{D}\gamma_\mu L\, V_2^\mu + y'\, \bar{Q}\gamma_\mu E\, V_2^\mu + y''\, \bar{Q}\gamma_\mu U\, V_2^{\dagger\mu} + \text{h.c.} \tag{4.4b}$$

$$\mathscr{L}_{U_1} = y\, \bar{Q}\gamma_\mu L\, U_1^\mu + y_2\, \bar{D}\gamma_\mu E\, U_1^\mu + \text{h.c.} \tag{4.4c}$$

JHEP09(2017)010

	Spin	Quantum Number	Clean observables new physics in e	Clean observables new physics in μ	All observables
S_3	0	$(\bar{3},3,1/3)$	✓	✓	✓
R_2	0	$(3,2,7/6)$	✓		
$\tilde{R}_2$	0	$(3,2,1/6)$			
$\tilde{S}_1$	0	$(\bar{3},1,4/3)$	✓		
U_3	1	$(3,3,2/3)$	✓	✓	✓
V_2	1	$(\bar{3},2,5/6)$	✓		
U_1	1	$(\bar{3},1,2/3)$	✓	✓	✓

Table 3. Which lepto-quarks can reproduce which $b \to s\ell^+\ell^-$ anomalies.

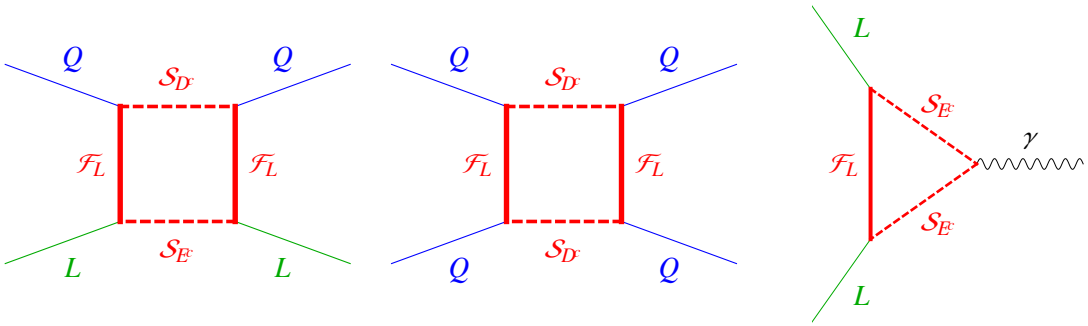

Figure 7. Feynman diagrams contributing to R_K, ΔM_{B_s} and the muon $g-2$ in models with extra fermions $\mathcal{F}$ and extra scalars $\mathcal{S}$. In Fundamental Composite Higgs models these diagrams will be dressed by further new composite dynamic contributions.

The vector LQ V_2 and U_1 can contribute to the anomalous observables trough multiple chiral structures. In general, if both y and y' are sizeable, dangerous scalar operators may be generated. If one of the two couplings dominates, we can again restrict to our one parameter fit, with the following correspondence: $C_{b_L\ell_L}$ can be generated by U_3; $C_{b_L\ell_R}$ or $C_{b_R\ell_L}$ can be generated by V_2; $C_{b_L\ell_L}$ or $C_{b_R\ell_R}$ can be generated by U_1.

Similar phenomenological considerations to explain the B-meson anomalies as in the case of the scalar LQ apply, we summarise the relevant options in table 3.

Models featuring vector LQs models in order to explain the flavour anomalies appeared recently in the literature [72–75], typically as new composite states. The presence of these states signals that the theory in isolation is non-renormalizable, meaning that loop effects of the vectors are UV divergent, for a recent re-discussion see ref. [76]. Naive dimensional analysis shows that one-loop contributions to physics observables such ΔM_{B_s} might be problematic. A careful study of this topic is a model dependent issue and it requires extra information on the UV embedding of the LQ in a complete theory.

JHEP09(2017)010

4.3 Models with loop mediators

The R_K anomaly can be reproduced by one loop diagrams involving new scalars $\mathcal{S}$ and new fermions $\mathcal{F}$ with Yukawa couplings to SM fermions that allow for the Feynman diagram on the left in figure 7 [39, 77] — see also ref. [78]. In this particular example, one generates an operator involving left-handed SM quarks and leptons, denoted respectively by Q and L. The needed extra Yukawa coupling to the muon must be large, $y_L \sim 1.5$. This also explains why the MSSM does not allow for an explanation of the R_K, R_{K^*} anomalies: a possibile box diagram containing Winos and sleptons predicts $y_L \sim g_2 \ll 1.5$, where g_2 is the $\mathrm{SU}(2)_L$ gauge coupling.

In section 4.4 we will consider renomalizable models of composite dynamics featuring extra elementary scalars, where we will show that the extra particles $\mathcal{S}$ and $\mathcal{F}$ can be identified with the constituents of the Higgs boson, and that their Yukawa couplings are the source of the SM Yukawa couplings, giving rise to a flavour structure similar to the SM structure. Then, the one loop Feynman diagrams of figure 7 are dressed by the underlying composite dynamic.

4.4 Fundamental composite Higgs

Models in which the Higgs is a composite state are prime candidates as potential source of new physics in the flavour sector [79–81]. Fundamental theories with a Higgs as a composite state that are also able to generate SM fermion masses appeared in ref. [82]. These theories feature both techni-scalars $\mathcal{S}$ and techni-fermions $\mathcal{F}$.[6] In models of fundamental composite Higgs: i) it is possible to replace the standard model Higgs and Yukawa sectors with a composite Higgs made of techni-particles; ii) the SM fermion masses are generated via a partial compositeness mechanism [66] in which the relevant composite techni-baryons emerge as bound states of a techni-fermion and a techni-scalar.

The composite theory does not address the SM naturalness issue and it is fundamental in the sense that it can be extrapolated till the Planck scale [82]. Having a fundamental theory of composite Higgs, we use it to investigate the flavour anomalies.

The gauge group and the field content of a simple model are summarised in table 4. Here the new strong group is chosen to be $\mathrm{SU}(N_{\mathrm{TC}})$ with $N_{\mathrm{TC}} = 3$ and we list the gauge quantum numbers of the new vectorial fermions and scalars that can provide a composite Higgs with Yukawa couplings to all SM fermions L, E, Q, U, D. Three generations of techni-scalars are introduced in order to reproduce all SM fermion masses and mixings, while having a renormalizable theory with no Landau poles below the Planck scale. The hypercharge Y of the $\mathcal{F}_L$ fermion is free. We assume the minimal choices $Y = -1/2$, $Y = 1/2$ and $Y = 0$.

The matrices of SM Yukawa couplings y_ℓ, y_{u}, y_{d} are obtained from the TC-Yukawa couplings

$$\mathscr{L}_Y = y_L\, L\mathcal{F}_L\mathcal{S}^*_{E^c} + y_E\, E\mathcal{F}^c_N\mathcal{S}_{E^c} + (y_D\, D\mathcal{F}^c_N + y_U\, U\mathcal{F}^c_{E^c})\mathcal{S}_{D^c} + y_Q\, Q\mathcal{F}_L\mathcal{S}^*_{D^c} + \mathrm{h.c.} \quad (4.5)$$

as $y_\ell \approx y_L y_E^T/g_{\mathrm{TC}}$, $y_{\mathrm{d}} \approx y_Q y_D^T/g_{\mathrm{TC}}$, $y_{\mathrm{u}} \approx y_Q y_U^T/g_{\mathrm{TC}}$, where the new gauge coupling g_{TC} becomes strong, $g_{\mathrm{TC}} \sim 4\pi/\sqrt{N_{\mathrm{TC}}}$, at the scale $\Lambda_{\mathrm{TC}} \sim g_{\mathrm{TC}} f_{\mathrm{TC}}$, forming composite particles

[6] Composite theories including TC scalars attempting to give masses to the SM quarks appeared earlier in the literature [83–88] for (walking) TC theories that didn't feature a light Higgs.

JHEP09(2017)010

name	spin	generations	$SU(3)_c$	$SU(2)_L$	$U(1)_Y$	$SU(3)_{TC}$
$\mathcal{F}_L$	1/2	1	1	2	$Y = -1/2$	3
$\mathcal{F}^c_N$	1/2	1	1	1	$-Y - 1/2 = 0$	3
$\mathcal{F}_{E^c}$	1/2	1	1	1	$Y - 1/2 = -1$	3
$\mathcal{S}_{E^c}$	0	3	1	1	$Y - 1/2 = -1$	3
$\mathcal{S}_{D^c}$	0	3	3	1	$Y + 1/6 = -1/3$	3

Table 4. Field content of the simplest Fundamental Composite Higgs model. Extra fermions $\mathcal{F}^c_N, \mathcal{F}_L, \mathcal{F}_{E^c}$ with conjugated gauge quantum numbers such that the fermion content is vectorial are implicit. Names are appropriate assuming the value $Y = -1/2$ for the hypercharge Y of $\mathcal{F}_L$; however generic values are allowed.

with mass of order $\Lambda_{\rm TC}$ and condensates $\langle \mathcal{F}\mathcal{F}^c \rangle \sim f^2_{\rm TC}\Lambda_{\rm TC}$. In view of the resulting breaking of the TC-chiral symmetry, the Higgs doublet H (identified with pseudo Goldstone bosons of the theory) and other composite scalars remain lighter. Lattice simulations [89–91] of the most minimal fundamental composite theories [92–94], without techni-scalars, have demonstrated the actual occurrence of chiral symmetry breaking with the relevant breaking pattern, and furthermore provided the spectrum of the spin one vector and axial techni-resonances with masses $m_V = 3.2(5)\,\mathrm{TeV}/\sin\theta$ and $m_A = 3.6(9)\,\mathrm{TeV}/\sin\theta$ where θ is the electroweak embedding angle to be determined by the dynamics, that must be smaller than about 0.2.

The TC-Yukawa couplings accidentally conserve lepton and baryon numbers (like in the SM) and TC-baryon number; depending on the value of Y the lightest TC-baryon can be a neutral DM candidate.

We require TC-scalar masses and TC-quartics to respect flavour symmetries so that the BSM corrections to flavour observables abide the experimental bounds. At one loop[7] in the TC-Yukawas one obtains the following operators involving 4 SM fermions

$$\sum_{f,f'}^{L,E,Q,U,D} \frac{(y_f^\dagger y_f)_{ij}(y_{f'}^\dagger y_{f'})_{i'j'}}{g^2_{\rm TC}\Lambda^2_{\rm TC}}(\bar{f}_i\gamma_\mu f'_{j'})(\bar{f}'_{i'}\gamma_\mu f_j) + \frac{(y_L^\dagger y_E^*)_{ij}(y_Q y_D^T)_{i'j'}}{g^2_{\rm TC}\Lambda^2_{\rm TC}}(\bar{L}_i\gamma_\mu Q_{i'})(\bar{E}_j\gamma_\mu D_{j'}). \tag{4.6}$$

All SM fermions and their chiralities are involved. These operators are phenomenologically viable if the fundamental TC-Yukawa couplings have the minimal values needed to reproduce the SM Yukawa couplings: $y_E \sim y_L \sim \sqrt{g_{\rm TC} y_\ell}$, and similarly for quarks.

However, when the TC-Yukawas (say, y_L) are enhanced the impact on new physics is also enhanced. The observed SM Yukawa couplings are reproduced when the corresponding TC-Yukawas (say, y_E) are reduced. Consequently, in this scenario new physics manifests prevalently in leptons of one given chirality. Because data prefer new physics to emerge prevalently in left-handed muons it is natural to consider here an enhanced muon coupling y_L and a correspondingly reduced right-handed y_E.

[7] The loop analysis, in the composite scenario, is merely a schematic way to keep track of the relevant factors stemming from the TC dynamics when writing SM four-fermion interactions.

JHEP09(2017)010

Coefficient	One-loop result	Non-perturbative estimate
$c_{b_L\mu_L}$	$N_{\rm TC}\dfrac{(y_L y_L^\dagger)_{\mu\mu}(y_Q y_Q^\dagger)_{bs}}{(4\pi)^2 4M^2_{\mathcal{F}_L}}F(x,y)$	$\dfrac{(y_L y_L^\dagger)_{\mu\mu}(y_Q y_Q^\dagger)_{bs}}{g^2_{\rm TC}\Lambda^2_{\rm TC}}$
$c_{b_L b_L}$	$N_{\rm TC}\dfrac{(y_Q y_Q^\dagger)^2_{bs}}{(4\pi)^2 8M^2_{\mathcal{F}_L}}F(x,x)$	$\dfrac{(y_Q y_Q^\dagger)^2_{bs}}{g^2_{\rm TC}\Lambda^2_{\rm TC}}$
Δa_μ	$N_{\rm TC}\dfrac{m^2_\mu (y_L y_L^\dagger)_{\mu\mu}}{(4\pi)^2 M^2_{\mathcal{F}_L}}\left[(2Y-1)F_7(y)+2Y\dfrac{F_7(1/y)}{y}\right]$	$\dfrac{m^2_\mu}{g_{\rm TC}\Lambda^2_{\rm TC}}$
$\delta g_{Z\mu_L}$	$N_{\rm TC}g_2\dfrac{M^2_Z (y_L y_L^\dagger)_{\mu\mu}}{2(4\pi)^2(1-2s^2_{\rm W})M^2_{\mathcal{F}_L}}\mathcal{F}_9(Y,y)$	$g_2\dfrac{M^2_Z (y_L y_L^\dagger)_{\mu\mu}}{g^2_{\rm TC}\Lambda^2_{\rm TC}}$

Table 5. Coefficients of the low-energy operators generated within a naive perturbative TC-fermion and TC-scalar estimate (second column) along with their NDA analysis counterpart (third column). The NDA result for Δa modifies in the presence of a TC-fermion condensate to $m_\mu v(y_L y_E^T)_{\mu\mu}/g_{\rm TC}\Lambda^2_{\rm TC}$.

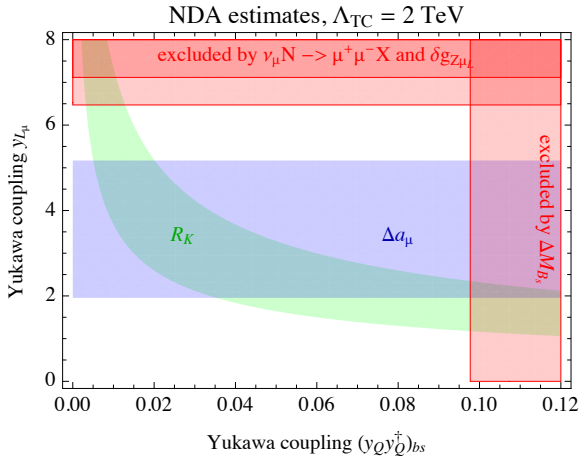

Figure 8. Estimates of signals and bounds on the Yukawa couplings of fundamental composite Higgs models. The model generates an effective operator that can simultaneously account for both R_K and R_{K^*}, so only R_K is plotted.

We summarise in table 5 the coefficients of the relevant flavour-violating effective operators, both within a naive one-loop approximation (adopting the results from refs. [11, 39]) and Naive Dimensional Analysis (NDA) in the composite theory. We defined $x = M^2_{\mathcal{S}^c_D}/M^2_{\mathcal{F}_L}$, $y = M^2_{\mathcal{S}^c_E}/M^2_{\mathcal{F}_L}$ and the loop functions

$$F(x,y) = \frac{1}{(1-x)(1-y)} + \frac{x^2\ln x}{(1-x)^2(x-y)} + \frac{y^2\ln y}{(1-y)^2(y-x)} \tag{4.7a}$$

$$F_7(y) = \frac{y^3 - 6y^2 + 6y\ln y + 3y + 2}{12(1-y)^4}, \tag{4.7b}$$

JHEP09(2017)010

$$F_9(y) = \frac{-2y^3 + 6\ln y + 9y^2 - 18y + 11}{36(y-1)^4}\,, \tag{4.7c}$$

$$G_9(y) = \frac{7 - 36y + 45y^2 - 16y^3 + 6(2y-3)y^2\ln y}{36(y-1)^4}, \tag{4.7d}$$

$$\mathcal{F}_9(Y,y) = s_{\rm W}^2(2Y-1)F_9(y) - (1 - s_{\rm W}^2(2Y+1))G_9(y) \tag{4.7e}$$

that equal $F(1,1) = 1/3$, $F_7(1) = \tilde{F}_7(1) = 1/24$, $F_9(1) = -1/24$, $G_9(1) = 1/8$, for degenerate masses. The latter entry in table 5 is the correction to the Z coupling to left-handed muons g_{μ_L}, written in terms of the weak mixing angle $s_{\rm W} = \sin\theta_{\rm W}$. The LEP bound at the Z pole is $|\delta g_{Z\mu_L}| \leq 0.8\% \cdot g_2$ at 2σ [95]. We can neglect TC-penguin diagrams [11]. We can always work in a basis where $y_L = \mathrm{diag}(y_{L_e}, y_{L_\mu}, y_{L_\tau})$ is diagonal, such that $(y_L y_L^\dagger)_{\mu\mu} = y_{L_\mu}^2$.

Figure 8 shows that, in order to reproduce the $b \to s\ell^+\ell^-$ anomalies and the muon $g-2$ anomaly, a relatively large Yukawa coupling $y_{L_\mu} \sim 1.5$ is needed, like in models with perturbative extra fermions and scalars. In the composite model such values of TC-Yukawa coupling have natural sizes. This is corroborated by a RGE analysis for y_{L_μ} that features an extra contribution involving the $g_{\rm TC}$ gauge coupling:

$$(4\pi)^2 \frac{\partial y_{L_\mu}}{\partial \ln\mu} = \frac{N_{\rm TC}+3}{2} y_{L_\mu}^3 - 3\frac{N_{\rm TC}^2-1}{2N_{\rm TC}} g_{\rm TC}^2 y_{L_\mu}\,, \tag{4.8}$$

In the presence of the first term only, setting $N_{\rm TC} = 1$, the Yukawa coupling grows with energy. Perturbativity up to a scale $\Lambda_{\rm max}$ implies $|y_{L_\mu}| < 2\pi/\sqrt{\ln(\Lambda_{\rm max}/\,\mathrm{TeV})}$, with $|y_{L_\mu}| \approx 1$ for $\Lambda_{\rm max} \sim M_{\rm Pl}$. In the presence of the second term a larger $y_{L_\mu} \sim g_{\rm TC}$ is compatible with the requirement that all couplings can be extrapolated up to the Planck scale. This is similar to how the strong coupling g_3 allows for $y_t \approx 1$ in the SM. In the fundamental composite Higgs model, the large couplings y_t and y_{L_μ} contribute to the prediction for the Higgs mass parameter in terms of $\Lambda_{\rm TC}$.

Lepton-flavour violation is absent as long as the y_E matrix is diagonal in the same basis where y_L is diagonal. Then $y_\ell = y_{L_\ell} y_{E_\ell}/g_{\rm TC}$ for $\ell = \{e,\mu,\tau\}$. In general, there can be a flavour-violating mixing matrix in the lepton sector. In particular, the mixing angle $\theta_{e\mu}$ generates $\mu \to e\gamma$, but only when effects at higher order in the Yukawa couplings are included [82]. Focusing on effects enhanced by the large coupling y_{L_μ} one has

$$\mathrm{BR}(\mu\to e\gamma) \sim \frac{4\pi\alpha_{\rm em} v^6 y_{E_e}^2 y_{L_\mu}^6 \theta_{e\mu}^2}{g_{\rm TC}^6 m_\mu^2 \Lambda_{\rm TC}^4} \sim y_{E_e}^2 y_{L_\mu}^6 \theta_{e\mu}^2 \left(\frac{2\,\mathrm{TeV}}{\Lambda_{\rm TC}}\right)^4 \tag{4.9}$$

The experimental bound $\mathrm{BR}(\mu\to e\gamma) < 0.6\ 10^{-12}$ [96] is satisfied even for $\theta_{e\mu} \sim 1$ provided that in the electron sector too one has a large y_{L_e} and a small $y_{E_e} \sim y_e \sim 10^{-6}$.

Finally, we mention an effect that can enhance the new-physics correction to some flavour-violating operators. While the fermion condensates induced by the strong dynamics are known, the scalar condensates are not known (although perhaps they are computable, for example by dedicated lattice simulations). Possible scalar condensates could break the accidental flavour symmetry among scalars, leading to extra lighter composite pseudo-Goldstone bosons. The state made of $\mathcal{S}_{E^c}^* \mathcal{S}_{D^c}$ behaves as a lepto-quark: if light it would mediate at tree level some effective operators, analogously to the $\tilde{S}_1$ lepto-quark considered in section 4.2.

JHEP09(2017)010

5 Conclusions

We found that the new measurement of R_{K^*} together with R_K favours new physics in left-handed leptons. Furthermore, adding to the fit kinematical $b \to s\mu^+\mu^-$ distributions (affected by theoretical uncertainties), one finds that they favour similar deviations from the SM in left-handed muons. However, even if the experimental uncertainties on R_K, R_{K^*} will be reduced, a precise determination of the new-physics parameters will be prevented by the fact that these are no longer theoretically clean observables, if new physics really affects muons differently from electrons.

We next discussed possible theoretical interpretations of the anomaly. One can build models compatible with all other data:

- One extra Z' vector can give extra new-physics operators that involve all chiralities of SM leptons. The simplest possibility motivated by anomaly cancellation is a vectorial coupling to leptons. However, unless the Z' is savagely coupled to $\bar{b}s$ quarks, a Z' coupled to $\bar{s}s$ and $\bar{b}b$ is disfavoured by $pp \to Z' \to \mu^+\mu^-$ searches at LHC and other contraints.

- One lepto-quark tends to give effects in muons or electron only (in order to avoid large flavour violations), and only in one chirality.

- One can add extra fermions and scalars such that they mediate, at one loop level, the desired new physics. Their Yukawa coupling to muons must be larger than unity.

While the effective 4-fermion operators that can account for the $b \to s\ell^+\ell^-$ anomalies need to be suppressed by a scale $\sim 30\,\text{TeV}$, the actual new physics can be at a lower scale, with obvious consequences for direct observability at the LHC and for Higgs mass naturalness.

Acknowledgments

We thank Marina Marinkovic, Andrea Tesi and Elena Vigiani for useful discussions. We thank Javier Virto for further useful comments. The work of A.S. is supported by the ERC grant NEO-NAT, the one of F.S. is partially supported by the Danish National Research Foundation Grant DNRF:90, and the one of G. D'A. thanks Andrea Wulzer and the Lattice QCD group of CERN, and in particular Agostino Patella, for sharing their computing resources. R.T. is supported by the Swiss National Science Foundation under the grant CRSII2-160814 (Sinergia). R.T. thanks INFN Sezione di Genova for computing resources, Alessandro Brunengo for computing support, and David Straub for clarifications about the Flavio program.

A List of observables used in the global fit

In table 6 and 7 we summarize the observables used in addition to the 'clean' observables. All bins are treated in the experimental analyses as independent, even if overlapping. It is

JHEP09(2017)010

Angular observables	
Observable	$[q^2_{\text{min}}, q^2_{\text{max}}]$ [GeV^2]
LHCb $B \to K^*\mu\mu$ 2015 S [9]	
$\langle F_L \rangle(B^0 \to K^*\mu\mu)$	[1.1, 6], [15, 19], [0.1, 0.98], [1.1, 2.5], [2.5, 4], [4, 6], [15, 17], [17, 19]
$\langle S_3 \rangle(B^0 \to K^*\mu\mu)$	[1.1, 6], [15, 19], [0.1, 0.98], [1.1, 2.5], [2.5, 4], [4, 6], [15, 17], [17, 19]
$\langle S_4 \rangle(B^0 \to K^*\mu\mu)$	[1.1, 6], [15, 19], [0.1, 0.98], [1.1, 2.5], [2.5, 4], [4, 6], [15, 17], [17, 19]
$\langle S_5 \rangle(B^0 \to K^*\mu\mu)$	[1.1, 6], [15, 19], [0.1, 0.98], [1.1, 2.5], [2.5, 4], [4, 6], [15, 17], [17, 19]
$\langle S_7 \rangle(B^0 \to K^*\mu\mu)$	[1.1, 6], [15, 19], [0.1, 0.98], [1.1, 2.5], [2.5, 4], [4, 6], [15, 17], [17, 19]
$\langle S_8 \rangle(B^0 \to K^*\mu\mu)$	[1.1, 6], [15, 19], [0.1, 0.98], [1.1, 2.5], [2.5, 4], [4, 6], [15, 17], [17, 19]
$\langle S_9 \rangle(B^0 \to K^*\mu\mu)$	[1.1, 6], [15, 19], [0.1, 0.98], [1.1, 2.5], [2.5, 4], [4, 6], [15, 17], [17, 19]
$\langle A_{FB} \rangle(B^0 \to K^*\mu\mu)$	[1.1, 6], [15, 19], [0.1, 0.98], [1.1, 2.5], [2.5, 4], [4, 6], [15, 17], [17, 19]
CMS $B \to K^*\mu\mu$ 2017 [97]	
$\langle P_1 \rangle(B^0 \to K^*\mu\mu)$	[1, 2], [2, 4.3], [4.3, 6], [16, 19]
$\langle P'_5 \rangle(B^0 \to K^*\mu\mu)$	[1, 2], [2, 4.3], [4.3, 6], [16, 19]
ATLAS $B \to K^*\mu\mu$ 2017 [98]	
$\langle F_L \rangle(B^0 \to K^*\mu\mu)$	[0.04, 2], [2, 4], [4, 6], [0.04, 4], [1.1, 6], [0.04, 6]
$\langle S_3 \rangle(B^0 \to K^*\mu\mu)$	[0.04, 2], [2, 4], [4, 6], [0.04, 4], [1.1, 6], [0.04, 6]
$\langle S_4 \rangle(B^0 \to K^*\mu\mu)$	[0.04, 2], [2, 4], [4, 6], [0.04, 4], [1.1, 6], [0.04, 6]
$\langle S_5 \rangle(B^0 \to K^*\mu\mu)$	[0.04, 2], [2, 4], [4, 6], [0.04, 4], [1.1, 6], [0.04, 6]
$\langle S_7 \rangle(B^0 \to K^*\mu\mu)$	[0.04, 2], [2, 4], [4, 6], [0.04, 4], [1.1, 6], [0.04, 6]
$\langle S_8 \rangle(B^0 \to K^*\mu\mu)$	[0.04, 2], [2, 4], [4, 6], [0.04, 4], [1.1, 6], [0.04, 6]
$\langle P_1 \rangle(B^0 \to K^*\mu\mu)$	[0.04, 2], [2, 4], [4, 6], [0.04, 4], [1.1, 6], [0.04, 6]
$\langle P'_4 \rangle(B^0 \to K^*\mu\mu)$	[0.04, 2], [2, 4], [4, 6], [0.04, 4], [1.1, 6], [0.04, 6]
$\langle P'_5 \rangle(B^0 \to K^*\mu\mu)$	[0.04, 2], [2, 4], [4, 6], [0.04, 4], [1.1, 6], [0.04, 6]
$\langle P'_6 \rangle(B^0 \to K^*\mu\mu)$	[0.04, 2], [2, 4], [4, 6], [0.04, 4], [1.1, 6], [0.04, 6]
$\langle P'_8 \rangle(B^0 \to K^*\mu\mu)$	[0.04, 2], [2, 4], [4, 6], [0.04, 4], [1.1, 6], [0.04, 6]

Table 6. List of angular observables used in the global fit in addition to the 'clean' observables.

clear that a correlation should exists between measurements in overlapping bins, however this is not estimated by the experimental collaborations. For this reason we include in our fit the measurements in all relevant bins, even if overlapping, without including any correlation beyond the ones given in the experimental papers. Notice that, for instance in the case of the LHCb analysis [9], the result in the bin $[1.1, 6]\,\text{GeV}^2$ has a smaller error than the measurements in the bins $[1.1, 2.5], [2.5, 4], [4, 6]\,\text{GeV}^2$, even when the information from these three bins is combined. In fact, we verified that the bin $[1.1, 6]\,\text{GeV}^2$ has a stronger impact on our fits than the three smaller bins. This shows that even if the measurements are potentially largely correlated, the largest bin dominates the fit, so that the effect of the unknown correlation becomes negligible.

JHEP09(2017)010

Branching ratios	
Observable	$[q^2_{\text{min}}, q^2_{\text{max}}]$ [GeV^2]
LHCb $B^\pm \to K\mu\mu$ 2014 [5]	
$\frac{d}{dq^2}\text{BR}(B^\pm \to K\mu\mu)$	[0.1, 0.98], [1.1, 2], [2, 3], [3, 4], [4, 5], [5, 6], [15, 16], [16, 17], [17, 18], [18, 19], [19, 20], [20, 21], [21, 22], [1.1, 6], [15, 22]
LHCb $B^0 \to K\mu\mu$ 2014 [5]	
$\frac{d}{dq^2}\text{BR}(B^0 \to K\mu\mu)$	[0.1, 2], [2, 4], [4, 6], [15, 17], [17, 22], [1.1, 6], [15, 22]
LHCb $B^\pm \to Kee$ 2014 [4]	
$\frac{d}{dq^2}\text{BR}(B^\pm \to Kee)$	[1, 6]
LHCb $B^\pm \to K^*\mu\mu$ 2014 [5]	
$\frac{d}{dq^2}\text{BR}(B^\pm \to K^*\mu\mu)$	[0.1, 2], [2, 4], [4, 6], [15, 17], [17, 19], [1.1, 6], [15, 19]
LHCb $B^0 \to K^*\mu\mu$ 2016 [99]	
$\frac{d}{dq^2}\text{BR}(B^0 \to K^*\mu\mu)$	[0.1, 0.98], [1.1, 2.5], [2.5, 4], [4, 6], [15, 17], [17, 19], [1.1, 6], [15, 19]
LHCb $B_s \to \phi\mu\mu$ 2015 [6]	
$\frac{d}{dq^2}\text{BR}(B_s \to \phi\mu\mu)$	[0.1, 2], [2, 5], [15, 17], [17, 19], [1, 6], [15, 19]
BaBar $B \to X_s ll$ 2013 [100]	
$\frac{d}{dq^2}\text{BR}(B \to X_s\mu\mu)$	[1, 6], [0.1, 2], [2, 4.3], [4.3, 6.8], [14.2, 25]
$\frac{d}{dq^2}\text{BR}(B \to X_see)$	[1, 6], [0.1, 2], [2, 4.3], [4.3, 6.8], [14.2, 25]
$\frac{d}{dq^2}\text{BR}(B \to X_sll)$	[1, 6], [0.1, 2], [2, 4.3], [4.3, 6.8], [14.2, 25]
Belle $B \to X_s ll$ 2005 [101]	
$\frac{d}{dq^2}\text{BR}(B \to X_sll)$	[0.04, 1], [1, 6], [14.4, 25]

Table 7. List of differential branching ratios used in the global fit in addition to the 'clean' observables.

References

[1] LHCb collaboration, *Test of lepton universality with $B^0 \to K^{*0}\ell^+\ell^-$ decays*, *JHEP* **08** (2017) 055 [arXiv:1705.05802] [INSPIRE].

[2] G. Hiller and F. Krüger, *More model-independent analysis of $b \to s$ processes*, *Phys. Rev.* **D 69** (2004) 074020 [hep-ph/0310219] [INSPIRE].

[3] M. Bordone, G. Isidori and A. Pattori, *On the Standard Model predictions for R_K and R_{K^*}*, *Eur. Phys. J.* **C 76** (2016) 440 [arXiv:1605.07633] [INSPIRE].

[4] LHCb collaboration, *Test of lepton universality using $B^+ \to K^+\ell^+\ell^-$ decays*, *Phys. Rev. Lett.* **113** (2014) 151601 [arXiv:1406.6482] [INSPIRE].

[5] LHCb collaboration, *Differential branching fractions and isospin asymmetries of $B \to K^{(*)}\mu^+\mu^-$ decays*, *JHEP* **06** (2014) 133 [arXiv:1403.8044] [INSPIRE].

JHEP09(2017)010

[6] LHCb collaboration, *Angular analysis and differential branching fraction of the decay* $B_s^0 \to \phi\mu^+\mu^-$, *JHEP* **09** (2015) 179 [arXiv:1506.08777] [INSPIRE].

[7] S. Descotes-Genon, J. Matias, M. Ramon and J. Virto, *Implications from clean observables for the binned analysis of* $B \to K^*\mu^+\mu^-$ *at large recoil*, *JHEP* **01** (2013) 048 [arXiv:1207.2753] [INSPIRE].

[8] LHCb collaboration, *Measurement of form-factor-independent observables in the decay* $B^0 \to K^{*0}\mu^+\mu^-$, *Phys. Rev. Lett.* **111** (2013) 191801 [arXiv:1308.1707] [INSPIRE].

[9] LHCb collaboration, *Angular analysis of the* $B^0 \to K^{*0}\mu^+\mu^-$ *decay using* $3\,\text{fb}^{-1}$ *of integrated luminosity*, *JHEP* **02** (2016) 104 [arXiv:1512.04442] [INSPIRE].

[10] G. Hiller and M. Schmaltz, R_K *and future* $b \to s\ell\ell$ *physics beyond the Standard Model opportunities*, *Phys. Rev.* **D 90** (2014) 054014 [arXiv:1408.1627] [INSPIRE].

[11] D. Ghosh, M. Nardecchia and S.A. Renner, *Hint of lepton flavour non-universality in B meson decays*, *JHEP* **12** (2014) 131 [arXiv:1408.4097] [INSPIRE].

[12] W. Altmannshofer and D.M. Straub, *New physics in* $b \to s$ *transitions after LHC run* 1, *Eur. Phys. J.* **C 75** (2015) 382 [arXiv:1411.3161] [INSPIRE].

[13] S. Descotes-Genon, L. Hofer, J. Matias and J. Virto, *Global analysis of* $b \to s\ell\ell$ *anomalies*, *JHEP* **06** (2016) 092 [arXiv:1510.04239] [INSPIRE].

[14] A. Khodjamirian, T. Mannel, A.A. Pivovarov and Y.-M. Wang, *Charm-loop effect in* $B \to K^{(*)}\ell^+\ell^-$ *and* $B \to K^*\gamma$, *JHEP* **09** (2010) 089 [arXiv:1006.4945] [INSPIRE].

[15] M. Beylich, G. Buchalla and T. Feldmann, *Theory of* $B \to K^{(*)}\ell^+\ell^-$ *decays at high* q^2*: OPE and quark-hadron duality*, *Eur. Phys. J.* **C 71** (2011) 1635 [arXiv:1101.5118] [INSPIRE].

[16] A. Khodjamirian, T. Mannel and Y.M. Wang, $B \to K\ell^+\ell^-$ *decay at large hadronic recoil*, *JHEP* **02** (2013) 010 [arXiv:1211.0234] [INSPIRE].

[17] S. Jäger and J. Martin Camalich, *On* $B \to V\ell\ell$ *at small dilepton invariant mass, power corrections and new physics*, *JHEP* **05** (2013) 043 [arXiv:1212.2263] [INSPIRE].

[18] J. Lyon and R. Zwicky, *Resonances gone topsy turvy — the charm of QCD or new physics in* $b \to s\ell^+\ell^-$*?*, arXiv:1406.0566 [INSPIRE].

[19] S. Descotes-Genon, L. Hofer, J. Matias and J. Virto, *On the impact of power corrections in the prediction of* $B \to K^*\mu^+\mu^-$ *observables*, *JHEP* **12** (2014) 125 [arXiv:1407.8526] [INSPIRE].

[20] S. Jäger and J. Martin Camalich, *Reassessing the discovery potential of the* $B \to K^*\ell^+\ell^-$ *decays in the large-recoil region: SM challenges and BSM opportunities*, *Phys. Rev.* **D 93** (2016) 014028 [arXiv:1412.3183] [INSPIRE].

[21] M. Ciuchini et al., $B \to K^*\ell^+\ell^-$ *decays at large recoil in the Standard Model: a theoretical reappraisal*, *JHEP* **06** (2016) 116 [arXiv:1512.07157] [INSPIRE].

[22] B. Capdevila, S. Descotes-Genon, L. Hofer and J. Matias, *Hadronic uncertainties in* $B \to K^*\mu^+\mu^-$*: a state-of-the-art analysis*, *JHEP* **04** (2017) 016 [arXiv:1701.08672] [INSPIRE].

[23] V.G. Chobanova, T. Hurth, F. Mahmoudi, D. Martinez Santos and S. Neshatpour, *Large hadronic power corrections or new physics in the rare decay* $B \to K^*\mu^+\mu^-$*?*, *JHEP* **07** (2017) 025 [arXiv:1702.02234] [INSPIRE].

JHEP09(2017)010

[24] G. Hiller and M. Schmaltz, *Diagnosing lepton-nonuniversality in $b \to s\ell\ell$*, *JHEP* **02** (2015) 055 [arXiv:1411.4773] [INSPIRE].

[25] R. Alonso, B. Grinstein and J. Martin Camalich, SU(2) × U(1) *gauge invariance and the shape of new physics in rare B decays*, *Phys. Rev. Lett.* **113** (2014) 241802 [arXiv:1407.7044] [INSPIRE].

[26] T. Blake, M. Gersabeck, L. Hofer, S. Jäger, Z. Liu and R. Zwicky, *Round table: flavour anomalies in $b \to s\ell^+\ell^-$ processes*, *EPJ Web Conf.* **137** (2017) 01001 [arXiv:1703.10005] [INSPIRE].

[27] C. Bobeth, G. Hiller and G. Piranishvili, *CP asymmetries in $\bar{B} \to \bar{K}^*(\to \bar{K}\pi)\bar{\ell}\ell$ and untagged $\bar{B}_s$, $B_s \to \phi(\to K^+K^-)\bar{\ell}\ell$ decays at NLO*, *JHEP* **07** (2008) 106 [arXiv:0805.2525] [INSPIRE].

[28] C. Hambrock, G. Hiller, S. Schacht and R. Zwicky, *$B \to K^\star$ form factors from flavor data to QCD and back*, *Phys. Rev.* **D 89** (2014) 074014 [arXiv:1308.4379] [INSPIRE].

[29] W. Altmannshofer, P. Ball, A. Bharucha, A.J. Buras, D.M. Straub and M. Wick, *Symmetries and asymmetries of $B \to K^*\mu^+\mu^-$ decays in the Standard Model and beyond*, *JHEP* **01** (2009) 019 [arXiv:0811.1214] [INSPIRE].

[30] A. Paul and D.M. Straub, *Constraints on new physics from radiative B decays*, *JHEP* **04** (2017) 027 [arXiv:1608.02556] [INSPIRE].

[31] LHCb collaboration, *Measurement of the $B_s^0 \to \mu^+\mu^-$ branching fraction and effective lifetime and search for $B^0 \to \mu^+\mu^-$ decays*, *Phys. Rev. Lett.* **118** (2017) 191801 [arXiv:1703.05747] [INSPIRE].

[32] D. Straub et al., *Flavio*, https://zenodo.org/record/495090#.WPMUzFJ7FTY.

[33] BELLE collaboration, S. Wehle et al., *Lepton-flavor-dependent angular analysis of $B \to K^*\ell^+\ell^-$*, *Phys. Rev. Lett.* **118** (2017) 111801 [arXiv:1612.05014] [INSPIRE].

[34] S. Descotes-Genon, J. Matias and J. Virto, *Understanding the $B \to K^*\mu^+\mu^-$ anomaly*, *Phys. Rev.* **D 88** (2013) 074002 [arXiv:1307.5683] [INSPIRE].

[35] L.-S. Geng, B. Grinstein, S. Jäger, J. Martin Camalich, X.-L. Ren and R.-X. Shi, *Towards the discovery of new physics with lepton-universality ratios of $b \to s\ell\ell$ decays*, arXiv:1704.05446 [INSPIRE].

[36] W. Altmannshofer, P. Stangl and D.M. Straub, *Interpreting hints for lepton flavor universality violation*, arXiv:1704.05435 [INSPIRE].

[37] B. Capdevila, A. Crivellin, S. Descotes-Genon, J. Matias and J. Virto, *Patterns of new physics in $b \to s\ell^+\ell^-$ transitions in the light of recent data*, arXiv:1704.05340 [INSPIRE].

[38] D. Foreman-Mackey, D.W. Hogg, D. Lang and J. Goodman, *emcee: the MCMC hammer*, *Publ. Astron. Soc. Pac.* **125** (2013) 306 [arXiv:1202.3665] [INSPIRE].

[39] P. Arnan, L. Hofer, F. Mescia and A. Crivellin, *Loop effects of heavy new scalars and fermions in $b \to s\mu^+\mu^-$*, *JHEP* **04** (2017) 043 [arXiv:1608.07832] [INSPIRE].

[40] W. Altmannshofer, S. Gori, M. Pospelov and I. Yavin, *Neutrino trident production: a powerful probe of new physics with neutrino beams*, *Phys. Rev. Lett.* **113** (2014) 091801 [arXiv:1406.2332] [INSPIRE].

JHEP09(2017)010

[41] Muon g-2 collaboration, G.W. Bennett et al., *Final report of the muon E821 anomalous magnetic moment measurement at BNL*, *Phys. Rev.* **D 73** (2006) 072003 [hep-ex/0602035] [INSPIRE].

[42] R. Gauld, F. Goertz and U. Haisch, *An explicit Z'-boson explanation of the $B \to K^* \mu^+ \mu^-$ anomaly*, *JHEP* **01** (2014) 069 [arXiv:1310.1082] [INSPIRE].

[43] A.J. Buras, F. De Fazio and J. Girrbach, 331 *models facing new $b \to s\mu^+\mu^-$ data*, *JHEP* **02** (2014) 112 [arXiv:1311.6729] [INSPIRE].

[44] W. Altmannshofer, S. Gori, M. Pospelov and I. Yavin, *Quark flavor transitions in L_μ-L_τ models*, *Phys. Rev.* **D 89** (2014) 095033 [arXiv:1403.1269] [INSPIRE].

[45] A. Crivellin, G. D'Ambrosio and J. Heeck, *Explaining $h \to \mu^\pm \tau^\mp$, $B \to K^* \mu^+ \mu^-$ and $B \to K \mu^+ \mu^- / B \to K e^+ e^-$ in a two-Higgs-doublet model with gauged L_μ-L_τ*, *Phys. Rev. Lett.* **114** (2015) 151801 [arXiv:1501.00993] [INSPIRE].

[46] A. Crivellin, G. D'Ambrosio and J. Heeck, *Addressing the LHC flavor anomalies with horizontal gauge symmetries*, *Phys. Rev.* **D 91** (2015) 075006 [arXiv:1503.03477] [INSPIRE].

[47] C. Niehoff, P. Stangl and D.M. Straub, *Violation of lepton flavour universality in composite Higgs models*, *Phys. Lett.* **B 747** (2015) 182 [arXiv:1503.03865] [INSPIRE].

[48] A. Celis, J. Fuentes-Martin, M. Jung and H. Serodio, *Family nonuniversal Z' models with protected flavor-changing interactions*, *Phys. Rev.* **D 92** (2015) 015007 [arXiv:1505.03079] [INSPIRE].

[49] A. Greljo, G. Isidori and D. Marzocca, *On the breaking of lepton flavor universality in B decays*, *JHEP* **07** (2015) 142 [arXiv:1506.01705] [INSPIRE].

[50] W. Altmannshofer and I. Yavin, *Predictions for lepton flavor universality violation in rare B decays in models with gauged L_μ-L_τ*, *Phys. Rev.* **D 92** (2015) 075022 [arXiv:1508.07009] [INSPIRE].

[51] A. Falkowski, M. Nardecchia and R. Ziegler, *Lepton flavor non-universality in B-meson decays from a* U(2) *flavor model*, *JHEP* **11** (2015) 173 [arXiv:1509.01249] [INSPIRE].

[52] A. Carmona and F. Goertz, *Lepton flavor and nonuniversality from minimal composite Higgs setups*, *Phys. Rev. Lett.* **116** (2016) 251801 [arXiv:1510.07658] [INSPIRE].

[53] F. Goertz, J.F. Kamenik, A. Katz and M. Nardecchia, *Indirect constraints on the scalar di-photon resonance at the LHC*, *JHEP* **05** (2016) 187 [arXiv:1512.08500] [INSPIRE].

[54] C.-W. Chiang, X.-G. He and G. Valencia, *Z' model for $b \to s\ell\bar{\ell}$ flavor anomalies*, *Phys. Rev.* **D 93** (2016) 074003 [arXiv:1601.07328] [INSPIRE].

[55] D. Bečirević, O. Sumensari and R. Zukanovich Funchal, *Lepton flavor violation in exclusive $b \to s$ decays*, *Eur. Phys. J.* **C 76** (2016) 134 [arXiv:1602.00881] [INSPIRE].

[56] S.M. Boucenna, A. Celis, J. Fuentes-Martin, A. Vicente and J. Virto, *Non-Abelian gauge extensions for B-decay anomalies*, *Phys. Lett.* **B 760** (2016) 214 [arXiv:1604.03088] [INSPIRE].

[57] S.M. Boucenna, A. Celis, J. Fuentes-Martin, A. Vicente and J. Virto, *Phenomenology of an* SU(2) × SU(2) × U(1) *model with lepton-flavour non-universality*, *JHEP* **12** (2016) 059 [arXiv:1608.01349] [INSPIRE].

JHEP09(2017)010

[58] E. Megias, G. Panico, O. Pujolàs and M. Quirós, *A natural origin for the LHCb anomalies*, *JHEP* **09** (2016) 118 [arXiv:1608.02362] [INSPIRE].

[59] I. Garcia Garcia, *LHCb anomalies from a natural perspective*, *JHEP* **03** (2017) 040 [arXiv:1611.03507] [INSPIRE].

[60] P. Ko, Y. Omura, Y. Shigekami and C. Yu, *LHCb anomaly and B physics in flavored Z' models with flavored Higgs doublets*, *Phys. Rev.* **D 95** (2017) 115040 [arXiv:1702.08666] [INSPIRE].

[61] E. Megias, M. Quirós and L. Salas, *Lepton-flavor universality violation in R_K and $R_{D^{(*)}}$ from warped space*, *JHEP* **07** (2017) 102 [arXiv:1703.06019] [INSPIRE].

[62] B. Allanach, F.S. Queiroz, A. Strumia and S. Sun, *Z' models for the LHCb and $g-2$ muon anomalies*, *Phys. Rev.* **D 93** (2016) 055045 [*Erratum ibid.* **D 95** (2017) 119902] [arXiv:1511.07447] [INSPIRE].

[63] I. Doršner, S. Fajfer, A. Greljo, J.F. Kamenik and N. Košnik, *Physics of leptoquarks in precision experiments and at particle colliders*, *Phys. Rept.* **641** (2016) 1 [arXiv:1603.04993] [INSPIRE].

[64] B. Gripaios, M. Nardecchia and S.A. Renner, *Composite leptoquarks and anomalies in B-meson decays*, *JHEP* **05** (2015) 006 [arXiv:1412.1791] [INSPIRE].

[65] B. Gripaios, *Composite leptoquarks at the LHC*, *JHEP* **02** (2010) 045 [arXiv:0910.1789] [INSPIRE].

[66] D.B. Kaplan, *Flavor at SSC energies: a new mechanism for dynamically generated fermion masses*, *Nucl. Phys.* **B 365** (1991) 259 [INSPIRE].

[67] I. de Medeiros Varzielas and G. Hiller, *Clues for flavor from rare lepton and quark decays*, *JHEP* **06** (2015) 072 [arXiv:1503.01084] [INSPIRE].

[68] A. Crivellin, D. Müller and T. Ota, *Simultaneous explanation of $R(D^{(*)})$ and $b \to s\mu^+\mu^-$: the last scalar leptoquarks standing*, arXiv:1703.09226 [INSPIRE].

[69] B. Allanach, A. Alves, F.S. Queiroz, K. Sinha and A. Strumia, *Interpreting the CMS $\ell^+\ell^- jj+$ missing transverse energy excess with a leptoquark model*, *Phys. Rev.* **D 92** (2015) 055023 [arXiv:1501.03494] [INSPIRE].

[70] D. Bečirević, S. Fajfer and N. Košnik, *Lepton flavor nonuniversality in $b \to s\ell^+\ell^-$ processes*, *Phys. Rev.* **D 92** (2015) 014016 [arXiv:1503.09024] [INSPIRE].

[71] S. Sahoo and R. Mohanta, *Scalar leptoquarks and the rare B meson decays*, *Phys. Rev.* **D 91** (2015) 094019 [arXiv:1501.05193] [INSPIRE].

[72] R. Alonso, B. Grinstein and J. Martin Camalich, *Lepton universality violation and lepton flavor conservation in B-meson decays*, *JHEP* **10** (2015) 184 [arXiv:1505.05164] [INSPIRE].

[73] R. Barbieri, G. Isidori, A. Pattori and F. Senia, *Anomalies in B-decays and* U(2) *flavour symmetry*, *Eur. Phys. J.* **C 76** (2016) 67 [arXiv:1512.01560] [INSPIRE].

[74] S. Sahoo, R. Mohanta and A.K. Giri, *Explaining the R_K and $R_{D^{(*)}}$ anomalies with vector leptoquarks*, *Phys. Rev.* **D 95** (2017) 035027 [arXiv:1609.04367] [INSPIRE].

[75] R. Barbieri, C.W. Murphy and F. Senia, *B-decay anomalies in a composite leptoquark model*, *Eur. Phys. J.* **C 77** (2017) 8 [arXiv:1611.04930] [INSPIRE].

JHEP09(2017)010

[76] C. Biggio, M. Bordone, L. Di Luzio and G. Ridolfi, *Massive vectors and loop observables: the $g-2$ case*, *JHEP* **10** (2016) 002 [arXiv:1607.07621] [INSPIRE].

[77] B. Gripaios, M. Nardecchia and S.A. Renner, *Linear flavour violation and anomalies in B physics*, *JHEP* **06** (2016) 083 [arXiv:1509.05020] [INSPIRE].

[78] G. Bélanger, C. Delaunay and S. Westhoff, *A dark matter relic from muon anomalies*, *Phys. Rev.* **D 92** (2015) 055021 [arXiv:1507.06660] [INSPIRE].

[79] D.B. Kaplan and H. Georgi, SU(2) $\times$ U(1) *breaking by vacuum misalignment*, *Phys. Lett.* **B 136** (1984) 183 [INSPIRE].

[80] D.B. Kaplan, H. Georgi and S. Dimopoulos, *Composite Higgs scalars*, *Phys. Lett.* **B 136** (1984) 187 [INSPIRE].

[81] M.J. Dugan, H. Georgi and D.B. Kaplan, *Anatomy of a composite Higgs model*, *Nucl. Phys.* **B 254** (1985) 299 [INSPIRE].

[82] F. Sannino, A. Strumia, A. Tesi and E. Vigiani, *Fundamental partial compositeness*, *JHEP* **11** (2016) 029 [arXiv:1607.01659] [INSPIRE].

[83] A. Kagan, *Recent developments in bosonic technicolor*, in 15$^{\text{th}}$ *Johns Hopkins Workshop on Current Problems in Particle Theory: Particle Physics from Underground to Heaven*, Baltimore MD U.S.A., 26–28 August 1991 [INSPIRE].

[84] B.A. Dobrescu, *Fermion masses without Higgs: a supersymmetric technicolor model*, *Nucl. Phys.* **B 449** (1995) 462 [hep-ph/9504399] [INSPIRE].

[85] A.L. Kagan, *Implications of TeV flavor physics for the $\Delta I = 1/2$ rule and $BR_\ell(B)$*, *Phys. Rev.* **D 51** (1995) 6196 [hep-ph/9409215] [INSPIRE].

[86] M. Antola, S. Di Chiara, F. Sannino and K. Tuominen, *Minimal super technicolor*, *Eur. Phys. J.* **C 71** (2011) 1784 [arXiv:1001.2040] [INSPIRE].

[87] M. Antola, S. Di Chiara, F. Sannino and K. Tuominen, *Supersymmetric extension of technicolor & fermion mass generation*, *Nucl. Phys.* **B 864** (2012) 664 [arXiv:1111.1009] [INSPIRE].

[88] W. Altmannshofer, S. Gori, A.L. Kagan, L. Silvestrini and J. Zupan, *Uncovering mass generation through Higgs flavor violation*, *Phys. Rev.* **D 93** (2016) 031301 [arXiv:1507.07927] [INSPIRE].

[89] R. Lewis, C. Pica and F. Sannino, *Light asymmetric dark matter on the lattice:* SU(2) *technicolor with two fundamental flavors*, *Phys. Rev.* **D 85** (2012) 014504 [arXiv:1109.3513] [INSPIRE].

[90] A. Hietanen, R. Lewis, C. Pica and F. Sannino, *Fundamental composite Higgs dynamics on the lattice:* SU(2) *with two flavors*, *JHEP* **07** (2014) 116 [arXiv:1404.2794] [INSPIRE].

[91] R. Arthur, V. Drach, M. Hansen, A. Hietanen, C. Pica and F. Sannino, SU(2) *gauge theory with two fundamental flavors: a minimal template for model building*, *Phys. Rev.* **D 94** (2016) 094507 [arXiv:1602.06559] [INSPIRE].

[92] T.A. Ryttov and F. Sannino, *Ultra minimal technicolor and its dark matter TIMP*, *Phys. Rev.* **D 78** (2008) 115010 [arXiv:0809.0713] [INSPIRE].

[93] J. Galloway, J.A. Evans, M.A. Luty and R.A. Tacchi, *Minimal conformal technicolor and precision electroweak tests*, *JHEP* **10** (2010) 086 [arXiv:1001.1361] [INSPIRE].

JHEP09(2017)010

[94] G. Cacciapaglia and F. Sannino, *Fundamental composite (Goldstone) Higgs dynamics*, *JHEP* **04** (2014) 111 [arXiv:1402.0233] [INSPIRE].

[95] SLD Electroweak Group, DELPHI, ALEPH, SLD, SLD Heavy Flavour Group, OPAL, LEP Electroweak Working Group and L3 collaborations, S. Schael et al., *Precision electroweak measurements on the Z resonance*, *Phys. Rept.* **427** (2006) 257 [hep-ex/0509008] [INSPIRE].

[96] MEG collaboration, J. Adam et al., *New constraint on the existence of the $\mu^+ \to e^+\gamma$ decay*, *Phys. Rev. Lett.* **110** (2013) 201801 [arXiv:1303.0754] [INSPIRE].

[97] CMS collaboration, *Measurement of the P_1 and P_5' angular parameters of the decay $B^0 \to K^{*0}\mu^+\mu^-$ in proton-proton collisions at $\sqrt{s} = 8$ TeV*, CMS-PAS-BPH-15-008, CERN, Geneva Switzerland, (2015).

[98] ATLAS collaboration, *Angular analysis of $B_d^0 \to K^*\mu^+\mu^-$ decays in pp collisions at $\sqrt{s} = 8$ TeV with the ATLAS detector*, ATLAS-CONF-2017-023, CERN, Geneva Switzerland, (2017).

[99] LHCb collaboration, *Measurements of the S-wave fraction in $B^0 \to K^+\pi^-\mu^+\mu^-$ decays and the $B^0 \to K^*(892)^0\mu^+\mu^-$ differential branching fraction*, *JHEP* **11** (2016) 047 [arXiv:1606.04731] [INSPIRE].

[100] BaBar collaboration, J.P. Lees et al., *Measurement of the $B \to X_s\ell^+\ell^-$ branching fraction and search for direct CP-violation from a sum of exclusive final states*, *Phys. Rev. Lett.* **112** (2014) 211802 [arXiv:1312.5364] [INSPIRE].

[101] Belle collaboration, M. Iwasaki et al., *Improved measurement of the electroweak penguin process $B \to X_s\ell^+\ell^-$*, *Phys. Rev.* **D 72** (2005) 092005 [hep-ex/0503044] [INSPIRE].

JHEP09(2017)010